

# Magnetic Circular Dichroism Spectroscopy as a Probe of Geometric and Electronic Structure of Cobalt(II)-Substituted Proteins: Ground-State Zero-Field Splitting as a Coordination Number Indicator

James A. Larrabee,\* Christopher M. Alessi, Esi T. Asiedu, Justin O. Cook, Keith R. Hoerning, Lance J. Klingler, Gregory S. Okin, Stuart G. Santee, and Thomas L. Volkert

Contribution from the Department of Chemistry and Biochemistry, Middlebury College, Middlebury, Vermont 05753

Received October 11, 1996<sup>⊗</sup>

**Abstract:** Variable-temperature magnetic circular dichroism (VT MCD) is used as a probe of the ground-state electronic structure in Co(II)-substituted liver alcohol dehydrogenase, carbonic anhydrase, carboxypeptidase, substrate and inhibitor complexes of these enzymes, and four- and five-coordinate Co(II) model complexes. VT MCD was used to determine the magnitude of the ground-state zero-field splitting (ZFS) in these samples. The four-coordinate Co(II) species had ZFS's that ranged from 2.3 to 30 cm<sup>-1</sup> and the five-coordinate species had ZFS's that ranged from 2.7 to 98 cm<sup>-1</sup>, values which fall outside of the ranges previously suggested for distinguishing 4-coordinate and 5-coordinate Co(II) (Makinen, M. W.; Kuo, L. C.; Yim, M. B.; Wells, G. B.; Fukuyama, J. M.; Kim, J. E. *J. Am. Chem. Soc.* **1985**, *107*, 5245–5255). The magnitude of the ZFS is not very sensitive to ligand heterogeneity but can be very sensitive to bond angles. Since protein active sites are in general highly angularly distorted from ideal four- or five-coordinate geometries, ZFS is rendered useless as a sole indicator of coordination number in Co(II)-substituted proteins. The MCD and absorption (or diffuse reflectance) spectra and the values of the ZFS for the proteins and model compounds are used in angle overlap method (AOM) calculations. These calculations support the conclusion that there is significant overlap in the ranges of ZFS for four- and five-coordinate Co(II) compounds.

## Introduction

The structure and structural changes around the active-site metal are keys to understanding the catalytic chemistry of any metalloenzyme. A great number of zinc enzymes have a four-coordinate Zn(II) active site in the resting form.<sup>1,2</sup> Associative mechanisms can be proposed in which the enzyme–substrate complex is formed by the addition of the substrate to the coordination sphere of the zinc, forming five-coordinate Zn(II). Alternatively, mechanisms involving the substitution of one of the zinc ligands with substrate or the association of the substrate with one of the existing zinc ligands produce a four-coordinate complex, although the active site may be significantly distorted from the resting form. A simple and relatively rapid method for distinguishing transient five-coordinate Zn(II) species from transient four-coordinate Zn(II) species could contribute to our understanding of many zinc enzymes. Determination of coordination number is of paramount importance to distinguish these two basic types of mechanisms.

Zn(II) cations are d<sup>10</sup>, closed shell, and not accessible to electronic spectroscopic probes, but Co(II) with a d<sup>7</sup> configuration can be substituted for Zn(II), creating an active site suitable for a variety of spectroscopic studies. Co(II) is similar in both size and coordination chemistry to Zn(II), so for most Co(II)-substituted zinc proteins partial or complete enzymatic activity is retained.<sup>2</sup> Furthermore high-resolution crystal structures of the native and Co(II) derivatives of carboxypeptidase (CPA and CoCPA) and horse liver alcohol dehydrogenase

(LADH and CoLADH) show that there are minimal protein or active-site structural differences induced by Co(II). Thus structural and mechanistic conclusions derived from study of active Co(II) derivatives may be reasonably applied to the native Zn(II) enzyme.<sup>2</sup>

Electronic absorption, circular dichroism (CD), and magnetic circular dichroism (MCD) data on simple Co(II) complexes which possess ideal four-coordinate (*T<sub>d</sub>*), ideal five-coordinate (*C<sub>4v</sub>* or *D<sub>3h</sub>*), or ideal six-coordinate (*O<sub>h</sub>*) geometries suggest that the pattern and intensities of the spectra are reliable indicators of coordination number.<sup>1,2</sup> However the CA, CPA, and LADH active sites are angularly distorted from ideal *T<sub>d</sub>* and have heterogeneous ligand fields.<sup>3–11</sup> Under these circumstances distinguishing four-coordinate from five-coordinate Co(II) using the pattern and intensity of electronic spectra becomes problematic.

(3) Eriksson, A. E.; Jones, T. A.; Liljas, A. *Proteins: Struct. Funct. Genet.* **1988**, *4*, 274–282.

(4) Vidgren, J.; Liljas, A.; Walker, N. P. C. *Int. J. Biol. Macromol.* **1990**, *12*, 342–344.

(5) Eriksson, A. E.; Kylsten, P. M.; Jones, T. A.; Liljas, A. *Proteins: Struct. Funct. Genet.* **1988**, *4*, 283–293.

(6) Brookhaven Protein Database, 1996.

(7) Hardman, K. D.; Lipscomb, W. N. *J. Am. Chem. Soc.* **1984**, *106*, 463–464.

(8) Rees, D. C.; Howard, J. B.; Chakrabarti, P.; Yeates, T.; Hsu, B. T.; Hardman, K. D.; Lipscomb, W. N. *Zinc Enzymes*; Bertini, I., Luchinat, C., Maret, W., Zeppezauer, M., Eds.; Birkhauser: Boston, 1986; Vol. 1, pp 155–166.

(9) Mangani, S.; Carloni, P.; Orioli, P. *J. Mol. Biol.* **1992**, *223*, 573–578.

(10) Schneider, G.; Eklund, H.; Cedergren-Zeppezauer, E.; Zeppezauer, M. *Proc Natl. Acad. Sci. USA* **1983**, *80*, 5289–5293.

(11) Cedergren-Zeppezauer, E. In *Zinc Enzymes*; Bertini, I., Luchinat, C., Maret, W., Zeppezauer, M., Eds.; Birkhauser: Boston, 1986; Vol. 1, pp 393–415.

<sup>⊗</sup> Abstract published in *Advance ACS Abstracts*, April 15, 1997.

(1) Bertini, I.; Luchinat, C. *Bioinorganic Chemistry*; Bertini, I., Gray, H. B., Lippard, S. J., Valentine, J. S., Eds.; University Science Books: Mill Valley, CA, 1994; pp 37–106.

(2) Maret, W.; Vallee, B. L. *Methods Enzymol.* **1993**, *226*, 52–65.

Clearly a single, reliable coordination number indicator for Co(II) that is applicable to resting as well as substrate and inhibitor complexes of the enzyme would be ideal. In the early to mid 1980s Makinen and co-workers used the temperature dependence of the cw saturation behavior of an electron paramagnetic resonance (EPR) signal (Orbach process) to measure the zero-field splitting (ZFS) of a series of small Co(II) compounds and the Co(II)-substituted zinc enzymes, CoCPA and CoLADH.<sup>12–14</sup> They claimed that the ZFS of the high-spin Co(II) ground state could be correlated with coordination number and could be used as a coordination number indicator (this correlation will henceforth be referred to as the CN/ZFS correlation). In the CN/ZFS correlation, four-coordinate Co(II) has a ZFS < 13 cm<sup>-1</sup>, five-coordinate Co(II) has a ZFS between 20 and 50 cm<sup>-1</sup>, and six-coordinate Co(II) has a ZFS > 50 cm<sup>-1</sup>. In the case of Co(II)-substituted zinc proteins, the distinction between four- and five-coordinate is more important, as six-coordinate Co(II) is not known in the resting state or postulated in any of the enzyme–substrate complexes of CoCA, CoCPA, or CoLADH.

In four- or five-coordinate Co(II) compounds ZFS is the splitting of the <sup>4</sup>A<sub>2</sub> (in *T<sub>d</sub>*), <sup>4</sup>A<sub>2</sub> (in *C<sub>4v</sub>*) or <sup>4</sup>A<sub>2</sub>' (in *D<sub>3h</sub>*) ground state into a pair of Kramer's doublets ( $m_J = \pm^{3/2}$  and  $m_J = \pm^{1/2}$ ), predominantly through second-order spin–orbit coupling with a higher lying state.<sup>15</sup> In the absence of any ligand field distortion from ideal geometry, spin–orbit coupling cannot occur between the <sup>4</sup>A<sub>2</sub> ground state and the <sup>4</sup>T<sub>2</sub>(F) first excited state in *T<sub>d</sub>* complexes, so the ZFS is zero, but with a small distortion from ideal *T<sub>d</sub>* symmetry, one would expect a small ZFS. In five-coordinate complexes, in either ideal geometry, low-lying <sup>4</sup>E states exist and can couple to the ground states via second-order spin–orbit coupling, even in the absence of any distortions. In six-coordinate, *O<sub>h</sub>*, complexes of Co(II), the ground state is <sup>4</sup>T<sub>1g</sub> which is subject to in-state (first-order) spin–orbit coupling, giving rise to a large ZFS. Qualitatively one would then expect the magnitude of ZFS to follow the order six-coordinate > five-coordinate > four-coordinate, and this is the basis for the CN/ZFS correlation. ZFS can also have signature. The sign convention for ZFS is that it is negative when the  $m_J = \pm^{3/2}$  is the lower energy doublet and positive when the  $m_J = \pm^{1/2}$  is the lower energy doublet; however, certain distortions which lower the symmetry of a molecule from *T<sub>d</sub>* will mix the  $m_J = \pm^{3/2}$  and  $m_J = \pm^{1/2}$  states making the sign of the ZFS ambiguous. In the absence of any symmetry, the  $m_J = \pm^{3/2}$  and  $m_J = \pm^{1/2}$  states completely mix, and  $m_J$  is no longer a “good” quantum number.

ZFS appeared to be a nearly ideal coordination number indicator that would have broad applications in mechanistic studies of Co(II)-substituted proteins. However Werth and co-workers, using variable-temperature magnetic circular dichroism at low applied magnetic fields (VT MCD) to determine the ZFS in CoLADH, have recently refuted the CN/ZFS correlation.<sup>16</sup> Werth *et al.* measured the ZFS for the very severely distorted catalytic active site in CoLADH to be 33 cm<sup>-1</sup>. This site is known to be four-coordinate from crystallography, but the ZFS is solidly in the five-coordinate range according to the CN/ZFS correlation.

We are interested in applying the technique of VT MCD to mononuclear and binuclear Co(II)-substituted proteins of unknown structure, so it is important to us to resolve the issue of a ZFS correlation with coordination number in Co(II) compounds. In order to address this issue we report the MCD spectra and the ZFS obtained by VT MCD for structurally characterized CoLADH, CoCA, CoCPA, and a number of their inhibitor and substrate complexes. There is always a possibility that the coordination around the Co(II) could change between the room-temperature single crystal and the low-temperature solution used in VT MCD, so a series of four- and five-coordinate Co(II) model compounds were also studied in the solid state and in solution. Our results were checked for consistency using angle overlap method (AOM) ligand field calculations.<sup>17,18</sup> These calculations provide a simple theoretical framework in which to understand the ZFS values through the electronic and physical structures of the molecules.

## Experimental Section

**Protein Samples.** Horse liver alcohol dehydrogenase (LADH, EC 1.1.1.1) was obtained from either Sigma Chemical Company (St. Louis, MO, Sigma number A-6128) or Boehringer (Mannheim, Germany). LADH was selectively substituted with Co(II) in either the catalytic site (Co(c)Zn(n)LADH) or noncatalytic site (Zn(c)Co(n)LADH) according to Zeppezauer *et al.*<sup>19,20</sup> in 50 mM TES/Na<sup>+</sup> buffer, pH 6.9 at 4 °C. The Co(c)Zn(n)LADH/NAD<sup>+</sup>/pyrazole complex was prepared in 50 mM TRIS/Cl<sup>-</sup> buffer, pH 7.5, according to Werth *et al.*<sup>16</sup> with 5 mM NAD<sup>+</sup> and 20 mM pyrazole. Samples were concentrated by centrifugation using Centricon-10, 10 000 MW cut-off micro concentrators (Amicon, Beverly, MA). Protein concentrations were determined by absorbance at 280 nm using  $\epsilon = 22\ 400\ \text{M}^{-1}\ \text{cm}^{-1}$  based on subunit concentration with each subunit being taken as 40 000 g/mol.

Bovine erythrocytes carbonic anhydrase (CA, EC 4.2.1.1) was obtained from Sigma Chemical Company (C-3934). The protein was purified on a DEAE Sephadex A-50 column to remove any residual hemoglobin.<sup>21</sup> Zinc was removed and cobalt(II) substituted according to published procedures.<sup>22,23</sup> High pH CoCA was prepared by dialysis against 50 mM HEPES/Na<sup>+</sup> buffer, pH 8.4 (chloride-free buffer, to avoid possible Cl<sup>-</sup> binding to the active site<sup>1</sup>) or in 50 mM TRIS/Cl<sup>-</sup> buffer, pH 9.0, and low pH CoCA was prepared by dialysis against 20 mM MES buffer, pH 5.9 containing 2 mM CoSO<sub>4</sub>. Protein samples were concentrated by centrifugation using Centricon-10, 10 000 MW cut-off micro concentrators. CA concentrations were determined by absorbance at 280 nm using  $\epsilon = 54\ 000\ \text{M}^{-1}\ \text{cm}^{-1}$ . CoCA concentrations were determined by absorbance at 640 nm for high pH CoCA ( $\epsilon = 178\ \text{M}^{-1}\ \text{cm}^{-1}$ ) and absorbance at 555 nm for low pH CoCA ( $\epsilon = 340\ \text{M}^{-1}\ \text{cm}^{-1}$ ).<sup>22</sup> CoCA inhibitor complexes were prepared by either direct addition of the inhibitor to a solution of the protein or by dialysis of the protein in a solution of the inhibitor. The correct inhibitor complex was verified by comparison to a published absorption spectrum.<sup>24</sup>

Bovine pancreas carboxypeptidase A (CPA, EC 3.4.17.1) was obtained from Sigma Chemical Company (C-0261). CoCPA was

(12) Makinen, M. W.; Kuo, L. C.; Yim, M. B.; Wells, G. B.; Fukuyama, J. M.; Kim, J. E. *J. Am. Chem. Soc.* **1985**, *107*, 5245–5255.

(13) Kuo, L. C.; Makinen, M. W. *J. Am. Chem. Soc.* **1985**, *107*, 5255–5261.

(14) Makinen, M. W.; Yim, M. B. *Proc. Natl. Acad. Sci. USA* **1981**, *78*, 6221–6225.

(15) Figgis, B. N. *Introduction to Ligand Fields*; Interscience: New York, 1966; pp 60, 296.

(16) Werth, M. T.; Tang, S-F.; Formicka, G.; Zeppezauer, M.; Johnson, M. K. *Inorg. Chem.* **1995**, *34*, 218–228.

(17) (a) Lever, A. B. P. *Inorganic Electronic Spectroscopy*, 2nd ed., Elsevier: Amsterdam, 1984; pp 53–74. (b) Banci, L.; Bencini, A.; Benelli, C.; Gatteschi, D.; Zanchini, C. *Struct. Bond.* **1982**, *52*, 37–86.

(18) Hoggard, P. E. in *Topics in Current Chemistry*; Springer-Verlag: Berlin, 1994; Vol. 171, pp 113–141. The AOMX program is available free and is maintained and documented by H. Adamsky, Institut für Theoretische Chemie, Heinrich-Heine-Universität, Düsseldorf, Germany; e-mail at adamsky@theochem.uni-duesseldorf.de.

(19) Maret, W.; Andersson, I.; Dietrich, H.; Schneider-Bernlohr, H.; Einarsson, R.; Zeppezauer, M. *Eur. J. Biochem.* **1979**, *98*, 501–512.

(20) Formicka-Kozłowska, G.; Zeppezauer, M. *Inorg. Chim. Acta* **1988**, *151*, 183–189.

(21) Armstrong, J. McD.; Myers, D. V.; Verpoorte, J. A., Edsall, J. T. *J. Biol. Chem.* **1966**, *241*, 5137–5149.

(22) Coleman, J. E. *Biochemistry* **1965**, *4*, 2644–2655.

(23) Pocker, Y.; Fong, T. O. *Biochemistry* **1980**, *19*, 2045–2050.

(24) Bertini, I.; Canti, G.; Luchinat, C.; Scozzafava, A. *J. Am. Chem. Soc.* **1978**, *100*, 4873–4877.

prepared according to Vallee *et al.*<sup>25</sup> Protein samples were concentrated by centrifugation using Centricon-10, 10 000 MW cut-off micro concentrators. CPA concentrations were determined by absorbance at 280 nm using  $\epsilon = 64\,200\text{ M}^{-1}\text{ cm}^{-1}$ . CoCPA concentrations were determined by absorbance at 550 nm for high pH CoCA ( $\epsilon = 155\text{ M}^{-1}\text{ cm}^{-1}$ ). CoCPA inhibitor complexes were prepared by either direct addition of the inhibitor to a solution of the protein or by dialysis of the protein in a solution of the inhibitor. The correct inhibitor complex was verified by comparison to a published absorption spectrum.<sup>25</sup>

**Model Compounds.** The following compounds were synthesized according to the published procedures given in each reference: bis-[( $\beta$ -mercapto- $\beta'$ , $\beta''$ -dimethylethyl)amino]cobalt(II), Co[SC(CH<sub>3</sub>)<sub>2</sub>CH<sub>2</sub>NH<sub>2</sub>]<sub>2</sub>;<sup>26</sup> Bis(2,2'-di(2-imidazolylbiphenyl)cobalt(II) diperchlorate triethanolate;<sup>27</sup> Co(imidazole)<sub>2</sub>Cl<sub>2</sub>;<sup>28</sup> Co(2-methylimidazole)<sub>4</sub>(ClO<sub>4</sub>)<sub>2</sub> and Co(2-methylimidazole)<sub>4</sub>(BF<sub>4</sub>)<sub>2</sub>;<sup>29</sup> Co(OH)<sub>4</sub><sup>2-</sup>;<sup>30</sup> Co(thiourea)<sub>2</sub>Cl<sub>2</sub>, [Co(thiourea)<sub>4</sub>](ClO<sub>4</sub>)<sub>2</sub>, and Co(thiourea)<sub>3</sub>SO<sub>4</sub>;<sup>31</sup> [Co(*N,N,N',N'*-tetraethyl-diethylenetriamine)Cl]Cl, Co(Et<sub>4</sub>dien)Cl<sub>2</sub>;<sup>32,33</sup> [Co(tris[2-(dimethylamino)ethyl]amine)Cl]Cl, [Co(Me<sub>6</sub>tren)Cl]Cl, and [Co(Me<sub>6</sub>tren)NCS]NCS;<sup>34</sup> Cs<sub>3</sub>CoCl<sub>5</sub> and Cs<sub>3</sub>CoBr<sub>5</sub>.<sup>35</sup> The following polypyrazolyl borate complexes of Co(II) were kindly provided by Drs. S. Trofimenko and J. S. Thompson of Du Pont, Wilmington, DE: Co(L<sub>1</sub>)(NCS), Co(L<sub>1</sub>)(NCO), Co(L<sub>1</sub>)(NO<sub>3</sub>) where L<sub>1</sub> = [HB(3-*tert*-butylpyrazole)<sub>3</sub>]<sup>-</sup>;<sup>36</sup> Co(L<sub>2</sub>)(Cl), Co(L<sub>2</sub>)(NCS) where L<sub>2</sub> = [HB(3-isopropyl-4-bromopyrazole)<sub>3</sub>]<sup>-</sup>;<sup>37</sup> Co(L<sub>2</sub>)(BBN(pz)<sub>2</sub>) where BBN(pz)<sub>2</sub> = 9-borabicyclo[3.3.1]nonane(pyrazole)<sub>2</sub>;<sup>38</sup> Co(L<sub>3</sub>)(N<sub>3</sub>), Co(L<sub>3</sub>)(NCO), Co(L<sub>3</sub>)(NCS), Co(L<sub>3</sub>)(NCS)(tetrahydrofuran) where L<sub>3</sub> = [HB(3-phenylpyrazole)<sub>3</sub>]<sup>-</sup>;<sup>36</sup> Co(B(3-isopropylpyrazole)<sub>4</sub>)<sub>2</sub>.<sup>37</sup>

**Physical Measurements.** Absorption spectra were taken using a OLIS-14 UV/vis/near-IR spectrophotometer. Diffuse reflectance spectra were recorded using an OLIS-17 UV/vis/near-IR spectrophotometer equipped with a Cary-17 integrating sphere diffuse reflectance accessory. For diffuse reflectance spectra, the sample was finely ground and mixed with magnesium oxide and the spectrum was recorded using pure magnesium oxide as a reference. MCD spectra were recorded on a JASCO J-600 spectropolarimeter equipped with an Oxford SM-4 4.0 T magnet/cryostat with an Oxford ITC-4 temperature controller. Temperatures were measured with a Lake Shore Cryogenics calibrated carbon/glass resistor located 2 mm from the sample. Solution samples were mixed with glycerol (50/50, v/v) and placed in a 0.5 cm pathlength brass sample cell with quartz windows. Solid samples were milled with poly(dimethylsiloxane) (Aldrich), squeezed between quartz windows, and held in a brass holder.

VT MCD data were collected by monitoring the CD signal at a given wavelength as a function of temperature and low applied magnetic field. The zero-field signal was used as the baseline. Strain that is introduced by freezing the glycerol solutions was estimated by the depolarization of the light beam. This was accomplished by measuring the difference in the CD spectrum intensity of a solution of nickel tartrate placed

before and after the sample in the cryostat.<sup>39</sup> If there were a 10% or more decrease in the intensity, the sample was thawed and refrozen. A change in the strain-induced depolarization during the course of the data collection causes an intensity change and is more important than the amount of depolarization; therefore, the intensity of the CD signal at a temperature of 4.22 K and a magnetic field of 0.5 T was checked for each sample at the beginning, middle, and end of each experimental run to make sure that the sample was not changing. Occasionally small shifts in the baselines were noted as the temperature was changed, but new baselines were collected at each temperature so this was not a problem. VT MCD was collected at the lowest possible magnetic fields (generally 0.1–0.5 T) to minimize the effects of field-induced mixing of states or crossing of two doublet states.<sup>40,41</sup> When the temperature of the sample was changed, the MCD intensities were not recorded until it was constant ( $\pm 0.02\text{ K}$ ) for 10 min.

**Calculations.** VT MCD data at a fixed low magnetic field were fit to<sup>40</sup>

$$\text{intensity} = \sum_i \left( \frac{C_i}{kT} \alpha_i H + B_i \alpha_i H \right) \quad (1)$$

where

$$\alpha_1 = \frac{1}{1 + e^{-\Delta/kT}}$$

and

$$\alpha_2 = \frac{e^{-\Delta/kT}}{1 + e^{-\Delta/kT}}$$

where  $C_i$  are the  $C$  term intensities for each state,  $B_i$  are the  $B$  term intensities for each state,  $k$  is Boltzmann's constant,  $\alpha_i$ 's are the Boltzmann population weighting factors,  $T$  is temperature in Kelvin, and  $H$  is the magnitude of the applied magnetic field.  $\Delta$  is the magnitude of the ZFS and includes both the axial and rhombic zero field splitting parameters as defined by<sup>16</sup>

$$\Delta = |2D[1 + 3(E/D)^2]^{1/2}| \quad (2)$$

where  $2D$  is the axial ZFS and  $E$  is the rhombic ZFS. The fit program that was actually used was originally written by J. McCormick in FORTRAN.<sup>41</sup> The fit using eq 1 is calculated using VT MCD data at only one magnetic field at a time. All of the parameters in eq 1 are allowed to float during the fit, but experimental estimates of  $B_0$  and  $C_0$  are made. The initial value of  $B_0$  is estimated experimentally from the change of the MCD intensity at 1.6 K between 3.8 and 4.0 T. At these conditions, only the lower doublet is giving rise to MCD intensity, and since the temperature dependent ( $C_0$  parameter) signal is saturated, changes in intensity associated with magnetic field changes are due only to the temperature-independent,  $B_0$ , parameter. After the  $B_0$  value is estimated, an estimate of the  $C_0$  parameter is made from the MCD intensity at 1.6 K. The values for the ZFS as well as the  $B_i$  and  $C_i$  parameters should not change significantly for different low magnetic fields, which was in fact observed. Relative standard deviations of the ZFS are generally 20% when based on an average of five values determined at magnetic fields of 0.1, 0.2, 0.3, 0.4, and 0.5 T.

Angle overlap method (AOM) calculations were made using AOMX, a FORTRAN program based on routines developed by Hoggard for  $d^3$  transition metal ions and extended to  $d^n$  systems by Adamsky.<sup>18</sup> AOMX fits were only attempted on proteins and compounds with available crystal structural data. During the fits the bond angles were not allowed to vary and the program was set up to calculate the best fit to the

- (25) Latt, S. A.; Vallee, B. L. *Biochemistry* **1971**, *10*, 4263–4270.  
 (26) Mastropaolo, D.; Thich, J. A.; Potenza, J. A.; Schugar, H. J. *J. Am. Chem. Soc.* **1977**, *99*, 424–429.  
 (27) Knapp, S.; Keenan, T. P.; Zhang, X.; Fikar, R.; Potenza, J. A.; Schugar, H. J. *J. Am. Chem. Soc.* **1990**, *112*, 3452–3464.  
 (28) Eilbeck, W.; Holmes, F.; Underhill, A. *J. Chem. Soc. A* **1967**, 757–761.  
 (29) Eilbeck, W. J.; Holmes, F.; Taylor, C. E.; Underhill, A. E. *J. Chem. Soc. A* **1968**, 128–132.  
 (30) Coleman, J. E.; Coleman, R. V. *J. Biol. Chem.* **1972**, *247*, 4718–4728.  
 (31) Cotton, F. A.; Faut, O. D.; Mague, J. T. *Inorg. Chem.* **1964**, *3*, 17–21.  
 (32) Dori, Z.; Eisenberg, R.; Gray, H. B. *Inorg. Chem.* **1967**, *6*, 483–486.  
 (33) Dori, Z.; Gray, H. B. *Inorg. Chem.* **1968**, *7*, 889–892.  
 (34) Ciampolini, M.; Nardi, N. *Inorg. Chem.* **1966**, *5*, 41–44.  
 (35) van Staple, R. P.; Belgers, H. G.; Bongers, P. F.; Zijlstra, H. J. *Chem. Phys.* **1966**, *44*, 3719–3725.  
 (36) Trofimenko, S.; Calabrese, J. C.; Thompson, J. S. *Inorg. Chem.* **1987**, *26*, 1507–1514.  
 (37) Trofimenko, S.; Calabrese, J. C.; Domaille, P. J.; Thompson, J. S. *Inorg. Chem.* **1989**, *28*, 1091–1101.  
 (38) Trofimenko, S.; Calabrese, J. C.; Thompson, J. S. *Inorg. Chem.* **1992**, *31*, 974–979.

- (39) Browett, W. R.; Fucaloro, A. F.; Morgan, T. V.; Stephens, P. J. *J. Am. Chem. Soc.* **1983**, *105*, 1868–1872.

- (40) Johnson, M. K. *Metal Clusters in Proteins*; Que, L., Jr., Ed.; American Chemical Society: Washington, DC, 1988; Vol. 372, pp 326–342.

- (41) Solomon, E. I.; Pavel, E. G.; Loeb, K. E.; Campochiaro, C. *Coord. Chem. Rev.* **1995**, *144*, 369–460. McCormick, J. M. Spectroscopic Studies of Mixed-Valent Binuclear Non-Heme Iron Active Sites. Ph.D. thesis, Stanford University, Stanford, CA, 1991.

observed d–d transition energies (absorption, diffuse reflectance, and/or MCD) and  $|\Delta|$  (ZFS) as determined by VT MCD by varying  $B$ ,  $C$  (Racah parameters),  $\zeta$  (spin–orbit coupling constant),  $\epsilon_\sigma$ , and  $\epsilon_\pi$ . For a perfect tetrahedron,  $\epsilon_\sigma$  and  $\epsilon_\pi$  are related to  $D_q$  by<sup>17</sup>

$$D_q = -2/15\epsilon_\sigma + 8/45\epsilon_\pi \quad (3)$$

Relationships of  $\epsilon_\sigma$  and  $\epsilon_\pi$  to other crystal field parameters such as  $D_s$ ,  $D_t$ ,  $DQ$ ,  $DT$  in different symmetries are given by Lever.<sup>17a</sup> In the AOMX calculations each experimental observable was given a weighting factor,  $W_i$ , which was calculated by

$$W_i = \frac{1}{\sigma^2(E_i)} \quad (4)$$

where  $\sigma$  is the estimate of the standard deviation of the observable and  $E_i$  is the value (energy) of the observable, either the band maximum in the absorption or MCD spectrum or the absolute value of the ZFS. The AOMX program minimizes the value of a fit function given by

$$\text{fit function} = \sqrt{\frac{\sum_i W_i (E_{i \text{ cal}} - E_{i \text{ obs}})^2}{n}} \quad (5)$$

where  $n$  is the number of observables. The standard deviation for d–d transitions was generally taken as the band width at half height of the MCD or absorption peak. The reason that such a high number was chosen is that AOMX assumes that the energies of the d–d bands are for the 0–0 transition. Since the compounds studied have broad vibronic envelopes, it is likely that the band maxima do not correspond to the 0–0 transitions. This introduces a small error in the values of the  $\epsilon_\sigma$ 's,  $\epsilon_\pi$ 's,  $\zeta$ 's, and Racah parameters. The weighting factors for the ZFS's were calculated using a 20% relative standard deviation.

Actual structural data were used, so none of the proteins or model complexes had any formal symmetry at all. The consequences of this require that precautions be taken to avoid misassigned bands in the AOMX calculations. A near-tetrahedral molecule has an absorption band in the visible region due to the d–d transition  ${}^4A_2 \rightarrow {}^4T_1(P)$ . Without any formal symmetry, the AOMX program calculates this transition to be composed of three spin–quartet transitions (all  ${}^4A \rightarrow {}^4A$ ) when spin–orbit coupling is “turned off” (by setting  $\zeta$  equal to zero). These transitions then split into six spin–doublet transitions when spin–orbit coupling is “turned on”. Because the d–d transitions are broad, even in the low temperature MCD spectrum, we never saw more than three transitions arising from the  ${}^4A_2 \rightarrow {}^4T_1(P)$  group. However there are a number of doublet transitions arising from the  ${}^2G$  free ion term near or overlapping in energy to the  ${}^4A_2 \rightarrow {}^4T_1(P)$  group. Thus when making band assignments in preparation for an AOMX calculation it is possible to misassign a “spin-allowed” band to a transition that is “spin-forbidden” if  $\zeta$  is allowed to be non-zero. To avoid making this error, a “prefit” AOMX calculation was always run first with  $\zeta$  set and held to zero. The value of the spin–orbit coupling constant had virtually no effect on the energies of the calculated transitions since the observed transitions were so broad. This yielded an initial set of AOM parameters ( $\epsilon_\sigma$ 's,  $B$ , and  $C$ ) based on minimizing the difference between the observed and calculated transition energies. In the final AOMX fits,  $\zeta$  was allowed to float and the experimental ZFS was included in the fit. There are no possible “spin-forbidden” transitions that could be mistaken for the near-infrared and infrared d–d transitions arising from the  ${}^4A_2 \rightarrow {}^4T_1(F)$  or  ${}^4A_2 \rightarrow {}^4T_2$  groups of bands.

AOMX was also used to calculate the ZFS for given “idealized” geometries and sets of typical ligand field parameters.

## Results

Table 1 summarizes the absolute values of the ZFS determined by VT MCD of the 13 four-coordinate Co(II)-substituted proteins or protein complexes, two five-coordinate Co(II)-substituted proteins or protein complexes, 19 four-coordinate Co(II) complexes, and six five-coordinate Co(II) complexes.

Three-quarters of these high-spin Co(II) examples had ZFS's that predicted the correct coordination number on the basis of the CN/ZFS correlation; however, 10 of 40 examples (those indicated by an asterisk) were found to have ZFS's outside of the ranges suggested by the CN/ZFS correlation for high-spin Co(II) compounds. Two four-coordinate examples were found to have a ZFS above  $13 \text{ cm}^{-1}$ . These were Co(c)Zn(n)LADH, having a ZFS of  $30 \text{ cm}^{-1}$ , and Co[SC(CH<sub>3</sub>)<sub>2</sub>CH<sub>2</sub>NH<sub>2</sub>]<sub>2</sub>, having a ZFS of  $21 \text{ cm}^{-1}$ . The geometries about the Co(II) in these two examples are such that the  $m_J = \pm 3/2$  and  $m_J = \pm 1/2$  levels mix (the Co(c)Zn(n)LADH has no local symmetry around the cobalt and the local symmetry around the cobalt in Co[SC(CH<sub>3</sub>)<sub>2</sub>CH<sub>2</sub>NH<sub>2</sub>]<sub>2</sub> is  $C_{2v}$ ), making the sign of the ZFS ambiguous and thus eliminating the argument that these may be negative and still fall in the correlation range for four-coordinate Co(II). Of the eight five-coordinate examples (six model compounds and two proteins), none of the measured ZFS's were in the 20–50  $\text{cm}^{-1}$  range. Seven of these were found to have a ZFS of less than  $20 \text{ cm}^{-1}$ , and the other had a ZFS of  $98 \text{ cm}^{-1}$ .

**Co Carbonic Anhydrase Derivatives.** Figure 1 shows the MCD and absorption spectra of bovine CoCA at pH 8.4. The inset in Figure 1 shows the fit of the VT MCD intensity data collected at  $544 \text{ nm}$  ( $18.4 \times 10^3 \text{ cm}^{-1}$ ) to eq 1. Table 2 summarizes the AOMX fit results for high-pH CoCA. The MCD and absorption spectra agree with those published by Coleman and Coleman<sup>30</sup> and the ZFS at  $3.6 \text{ cm}^{-1}$  is well within the correlation range for four-coordinate Co(II).<sup>12</sup> The AOMX results are based on the assignments suggested originally by Coleman and Coleman in which the bands at  $614 \text{ nm}$  ( $16.3 \times 10^3 \text{ cm}^{-1}$ ) and  $634 \text{ nm}$  ( $15.8 \times 10^3 \text{ cm}^{-1}$ ) are assigned to spin-forbidden (doublet) transitions.<sup>30</sup> These bands are quite intense in the absorption spectrum but are relatively weak in the MCD spectrum. With these assignments, the AOMX program calculated 10 d–d transitions and the ZFS within experimental error using only five parameters ( $\epsilon_\sigma(N)$ ,  $\epsilon_\sigma(O)$ ,  $B$ , and  $\zeta$ ;  $C$  is set to  $4.6B$ ) and the structure given by Eriksson *et al.* for the native zinc form of human carbonic anhydrase II.<sup>3</sup> The three imidazole nitrogens are at three different bond distances, but using three separate  $\epsilon_\sigma$ 's for these did not significantly improve the fit. Assignment of the bands at  $614$  and  $634 \text{ nm}$  to the  ${}^4A_2 \rightarrow {}^4T_1(P)$  group of bands, as has been suggested by the *ab initio* calculations of Garner and Krauss,<sup>42,43</sup> lead to a very poor AOMX fit. The calculated versus observed transition energies differ by 10% or more and the calculated  $\epsilon_\sigma(O)$  value for the water ligand is only  $690 \text{ cm}^{-1}$ , an unrealistically low value. Furthermore the resulting calculated ZFS was too high at  $7.5 \text{ cm}^{-1}$  even if a value of  $200 \text{ cm}^{-1}$  is used for  $\zeta$ .

Figure SI-1 (the SI prefix indicates that these figures have been deposited as Supporting Information) shows the MCD and absorption spectrum of the acetazolamide complex of bovine CoCA. The inset shows the fit of the VT MCD data at  $592 \text{ nm}$  ( $16.9 \times 10^3 \text{ cm}^{-1}$ , this wavelength was chosen so as to avoid any overlap with possible unreacted CoCA) to eq 1 to obtain a ZFS of  $11 \text{ cm}^{-1}$ . The ZFS has been measured on the human B CoCA/acetazolamide complex by magnetic susceptibility to be  $33 \text{ cm}^{-1}$ <sup>44</sup> and, on the basis of this value, was suggested to have five-coordinate Co(II).<sup>14</sup> The EPR  $g$ 's have also been used to determine a ZFS of  $17 \text{ cm}^{-1}$  for the human B CoCA/acetazolamide complex and  $13 \text{ cm}^{-1}$  for the bovine CoCA/acetazolamide complex,<sup>61</sup> closer to the  $11 \text{ cm}^{-1}$  ( $\pm 20\%$ )

(42) Garner, D. R.; Krauss, M. *Int. J. Quantum Chem.* **1992**, *42*, 1469–1477.

(43) Garner, D. R.; Krauss, M. *J. Am. Chem. Soc.* **1993**, *115*, 10247–10257.

(44) Aasa, R.; Hansen, M.; Lindskog, S. *Biochim. Biophys. Acta* **1976**, *453*, 211–217.

**Table 1.** Summary of the Absolute Values of Zero-Field Splitting Energies,  $|\Delta|$ , for Co(II)-Substituted Proteins and Model Compounds as Determined by VT-MCD

sample	Co(II) coordination no., first coordination sphere ligands		$ \Delta $ , cm <sup>-1</sup>		sample	Co(II) coordination no., first coordination sphere ligands		$ \Delta $ , cm <sup>-1</sup>	
	this work	literature	this work	literature		this work	literature		
Co(c)/Zn(m)LADH*	4, CoS <sub>2</sub> NO <sup>a</sup>	9.3, <sup>a</sup> 33 <sup>c</sup>	30		Proteins	4, CoN <sub>3</sub> NO <sup>k</sup>	3.5		
Zn(c)Co(m)LADH	4, CoS <sub>4</sub> <sup>d</sup>	7 <sup>c</sup>	3.3		CoCPA/gly-L-tyr	4, CoN <sub>2</sub> OO <sup>k</sup>	6.1		51 <sup>f</sup>
Co(c)/Zn(m)LADH/NAD <sup>+</sup> /pyrazole	4, CoS <sub>2</sub> NN <sup>d</sup>	47, <sup>b</sup> 56 <sup>e</sup>	4.8 (see text)		CoCPA/L-benzyl succinate	4, CoN <sub>2</sub> OO <sup>m</sup>	3.0		
CoCA (high pH)	4, CoN <sub>3</sub> O <sup>e</sup>		3.6		CoCPA/butyrate (low conc)	4, CoN <sub>2</sub> OO <sup>m</sup>	4.2		
CoCA/NCS <sup>-</sup>	5, CoN <sub>3</sub> NO <sup>e</sup>		5.7		CoCPA/butyrate (high conc)	4, CoN <sub>2</sub> OO <sup>m</sup>	3.7		
CoCA/acetazolamide	4, CoN <sub>3</sub> N <sup>f</sup>	13, <sup>g</sup> 17, <sup>h</sup> 33 <sup>i</sup>	11		CoCPA/phenyl acetate	4, CoN <sub>2</sub> OO <sup>m</sup>	4.0		
CoCA (low pH)*	5, CoN <sub>3</sub> O <sup>j</sup>		6.1		CoCPA/ $\beta$ -phenylpropionate (low conc)	4, CoN <sub>2</sub> OO <sup>m</sup>	4.1		
CoCPA	4, CoN <sub>2</sub> OO <sup>k</sup>	8.3 <sup>i</sup>	5.8		CoCPA/ $\beta$ -phenylpropionate (high conc)	4, CoN <sub>2</sub> OO <sup>m</sup>			
Co(OH) <sub>4</sub> <sup>2-</sup>	4, CoO <sub>4</sub> <sup>n</sup>		5.0		Four-Coordinate Model Compounds	4, CoN <sub>3</sub> N <sup>u</sup>	3.0		
Cs <sub>3</sub> CoCl <sub>5</sub>	4, CoCl <sub>4</sub> <sup>o</sup>	8.6 <sup>p</sup>	5.3		Co(L <sub>1</sub> )(NCO)	4, CoN <sub>3</sub> N <sup>v</sup>	3.7		
Cs <sub>3</sub> CoBr <sub>5</sub>	4, CoBr <sub>4</sub> <sup>o</sup>	10.68 <sup>p</sup>	6.6		Co(L <sub>2</sub> )(NCS)	4, CoN <sub>3</sub> Cl <sup>w</sup>	4.8		
Co(2-methylimidazole) <sub>4</sub> (ClO <sub>4</sub> ) <sub>2</sub>	4, CoN <sub>4</sub> <sup>q</sup>		5.1		Co(L <sub>2</sub> )Cl	4, CoN <sub>3</sub> N <sup>x</sup>	4.2		
Co(2-methylimidazole) <sub>4</sub> (BF <sub>4</sub> ) <sub>2</sub>	4, CoN <sub>4</sub> <sup>q</sup>		4.1		Co(L <sub>3</sub> (N <sub>3</sub> ))	4, CoN <sub>3</sub> N <sup>x</sup>	3.0		
Co(imidazole) <sub>2</sub> Cl <sub>2</sub>	4, CoN <sub>2</sub> Cl <sub>2</sub> <sup>r</sup>		5.3		Co(L <sub>3</sub> )(NCO)	4, CoN <sub>3</sub> N <sup>x</sup>	3.1		
Co(thiourea) <sub>2</sub> Cl <sub>2</sub>	4, CoS <sub>2</sub> Cl <sub>2</sub> <sup>s</sup>		4.9		Co(B-(3-isopropylpyrazole) <sub>4</sub> ) <sub>2</sub>	4, CoN <sub>4</sub> <sup>r</sup>	2.3		
Co(thiourea) <sub>3</sub> SO <sub>4</sub>	4, CoS <sub>3</sub> O <sup>s</sup>		5.6		Co[SC(CH <sub>3</sub> ) <sub>2</sub> CH <sub>2</sub> NH <sub>2</sub> ] <sub>2</sub> *	4, CoS <sub>2</sub> N <sub>2</sub> <sup>y</sup>	21		
Co(thiourea) <sub>4</sub> (ClO <sub>4</sub> ) <sub>2</sub>	4, CoS <sub>4</sub> <sup>t</sup>		3.8		bis(2,2'-di-2-imidazolylbiphenyl)cobalt(II)	4, CoN <sub>4</sub> <sup>r</sup>	5.6		
Co(L <sub>1</sub> )(NCS)	4, CoN <sub>3</sub> N <sup>r</sup>		3.7		dipерchlorate triethanolate				
					Five-Coordinate Model Compounds				
Co(Et <sub>2</sub> dien)Cl <sub>2</sub> *	5, CoN <sub>3</sub> Cl <sub>2</sub> <sup>aa</sup>		98		Co(L <sub>1</sub> )(NO <sub>3</sub> )*	5, CoN <sub>3</sub> O <sup>j</sup>	6.9		
[Co(Me <sub>6</sub> tren)Cl]Cl*	5, CoN <sub>4</sub> Cl <sup>bb</sup>		5.4		Co(L <sub>2</sub> )(BBN(pz) <sub>2</sub> )*	5, CoN <sub>3</sub> N <sub>2</sub> <sup>ff</sup>	16		
[Co(Me <sub>6</sub> tren)(NCS)](NCS)*	5, CoN <sub>4</sub> N <sup>ee</sup>		2.7		Co(L <sub>3</sub> )(NCS)(THF)*	5, CoN <sub>3</sub> NO <sup>f</sup>	14		

\* An asterisk indicates that the ZFS falls outside of the CN/ZFS correlation range. <sup>a</sup> From crystal structure. <sup>10</sup> <sup>b</sup> By EPR. <sup>14</sup> <sup>c</sup> By VT-MCD. <sup>16</sup> <sup>d</sup> From crystal structure. <sup>11</sup> <sup>e</sup> From crystal structure of human zinc form. <sup>3,5</sup> <sup>f</sup> From crystal structure of human zinc form. <sup>4</sup> <sup>g</sup> From EPR  $g$ 's on bovine CoCA/acetazolamide. <sup>61</sup> <sup>h</sup> From EPR  $g$ 's on human B CoCA/acetazolamide. <sup>61</sup> <sup>i</sup> By magnetic susceptibility on human B CoCA/acetazolamide. <sup>44</sup> <sup>j</sup> Putative coordination number from a variety of techniques, but not crystal structure. <sup>1</sup> <sup>k</sup> From crystal structure. <sup>6-9</sup> and XAFS. <sup>48</sup> <sup>l</sup> By EPR. <sup>13</sup> <sup>m</sup> By inference using absorption and MCD spectra. <sup>25</sup> <sup>n</sup> Spectroscopic. <sup>30,58</sup> <sup>o</sup> By crystal structure. <sup>35</sup> <sup>p</sup> By EPR. <sup>12,35</sup> <sup>q</sup> By crystal structure. <sup>35</sup> <sup>r</sup> By crystal structure. <sup>51</sup> <sup>s</sup> By crystal structure. <sup>52</sup> <sup>t</sup> By crystal structure. <sup>27</sup> <sup>aa</sup> By crystal structure. <sup>32</sup> and UV/vis. <sup>33</sup> <sup>bb</sup> By crystal structure. <sup>55</sup> <sup>cc</sup> From crystal structure. <sup>37</sup> <sup>ww</sup> By analogy with Co(L<sub>2</sub>)(NCS). <sup>3</sup> <sup>dd</sup> Calculated from near-IR band<sup>12</sup> using formula given by Wood. <sup>54</sup> <sup>ee</sup> By crystal structure. <sup>56</sup> <sup>ff</sup> By crystal structure. <sup>38</sup> <sup>gg</sup> By crystal structure. <sup>57</sup>

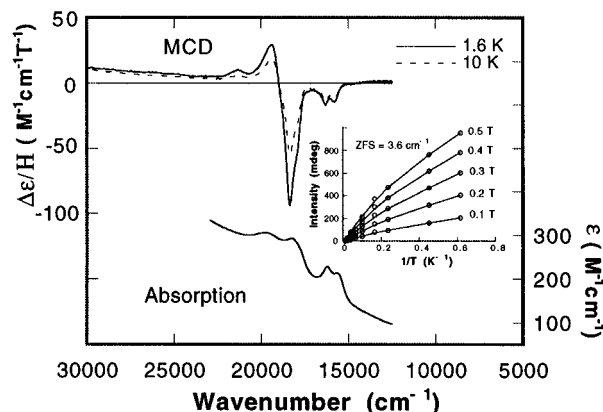


**Figure 1.** MCD spectra taken at 3.5 T of high pH CoCA, 0.47 mM CoCA in 50 mM HEPES/Na<sup>+</sup> buffer, pH 8.4, 70% (v/v) glycerol. Absorption spectrum is of the same sample taken after the MCD experiments. Inset is the fit of the VT MCD intensity data at  $18.4 \times 10^3 \text{ cm}^{-1}$  to eq 1. Open circles are the experimental data points, and the solid line is the calculated fit to eq 1. Fit parameters at 0.5 T:  $B_0 = 33$ ;  $C_0 = 1907$ ;  $B_1 = -121$ ;  $C_1 = 5305$ . Average ZFS at all five fields is  $3.6 \text{ cm}^{-1}$ .

**Table 2.** Summary of AOMX Calculation Results for Bovine CoCA<sup>a</sup>

derivative	origin in $T_d$	d-d transitions ( $\text{cm}^{-1}/1000$ )	
		observed	calculated
CoCA (high pH)	$^4A_2 \rightarrow ^4T_1(\text{F})$	8.2 <sup>24</sup>	8.3
	$^4A_2 \rightarrow ^4T_1(\text{F})$	11.0 <sup>24</sup>	10.9
	$^4A_2 \rightarrow ^2T_1, ^2E(\text{G})$	15.8 <sup>b</sup>	15.8
	$^4A_2 \rightarrow ^2T_1, ^2E(\text{G})$	16.3 <sup>b</sup>	16.2
	$^4A_2 \rightarrow ^4T_1(\text{P})$	17.9	17.8
	$^4A_2 \rightarrow ^4T_1(\text{P})$	18.4	18.4
	$^4A_2 \rightarrow ^4T_1(\text{P})$	19.4	19.4
	$^4A_2 \rightarrow ^2A_1, ^2T_2(\text{G})$	20.3 <sup>b</sup>	20.4
	$^4A_2 \rightarrow ^2A_1, ^2T_2(\text{G})$	20.8 <sup>b</sup>	21.0
	$^4A_2 \rightarrow ^2A_1, ^2T_2(\text{G})$	21.3 <sup>b</sup>	21.3
ZFS, $ \Delta $		3.6 $\text{cm}^{-1}$	3.3 $\text{cm}^{-1}$

<sup>a</sup> AOMX parameters ( $\text{cm}^{-1}$ ):  $\epsilon_\sigma(\text{N}) = 4640$  (one imidazole at 2.1 Å, 1 imidazole at 2.0 Å, 1 imidazole at 1.9 Å);  $\epsilon_\sigma(\text{O}) = 2040$  (one water at 2.1 Å);  $B = 774$ ;  $C = 4.6B$ ;  $\zeta = 252$ . <sup>b</sup> These assignments were first suggested by Coleman and Coleman.<sup>30</sup>

**Table 3.** Summary of AOMX Calculation Results for Bovine CoCA/Acetazolamide<sup>a</sup>

derivative	origin in $T_d$	d-d transitions ( $\text{cm}^{-1}/1000$ )	
		observed	calculated
CoCA/ acetazolamide	$^4A_2 \rightarrow ^4T_1(\text{F})$	7.9 <sup>24</sup>	8.5
	$^4A_2 \rightarrow ^4T_1(\text{F})$	9.2 <sup>24</sup>	9.2
	$^4A_2 \rightarrow ^4T_1(\text{F})$	11.0 <sup>24</sup>	10.6
	$^4A_2 \rightarrow ^2T_1, ^2E(\text{G})$	16.9	17.5
	$^4A_2 \rightarrow ^4T_1(\text{P})$	17.5	17.6
	$^4A_2 \rightarrow ^4T_1(\text{P})$	18.3	18.6
	$^4A_2 \rightarrow ^4T_1(\text{P})$	19.3	18.8
	$^4A_2 \rightarrow ^2A_1, ^2T_2(\text{G})$	21.5	21.5
	$^4A_2 \rightarrow ^2A_1, ^2T_2(\text{G})$	22.2	22.2
ZFS, $ \Delta $		11 $\text{cm}^{-1}$	11 $\text{cm}^{-1}$

<sup>a</sup> AOMX parameters ( $\text{cm}^{-1}$ ):  $\epsilon_\sigma(\text{N}) = 4270$  (three imidazoles at 2.0 Å);  $\epsilon_\sigma(\text{N}) = 4870$  (one sulfonamide nitrogen at 1.9 Å).  $B = 722$ ;  $C = 4.6B$ ;  $\zeta = 407$ .

value obtained by MCD. Table 3 summarizes the AOMX calculation results for CoCA/acetazolamide using the structure of the native zinc human carbonic anhydrase/acetazolamide complex reported by Vidgren *et al.*<sup>4</sup> In this structure, the acetazolamide has displaced the water ligand and is bound to the zinc through the sulfonamide nitrogen at 1.9 Å with the

**Table 4.** Summary of AOMX Calculation Results for Bovine CoCA/NCS<sup>-</sup>

derivative	origin in $C_{4v}$	d-d transitions ( $\text{cm}^{-1}/1000$ )	
		observed	calculated
CoCA/NCS <sup>-</sup>	$^4A_2 \rightarrow ^4E(\text{F})$	8.5 <sup>24</sup>	7.3
	$^4A_2 \rightarrow ^4E(\text{F})$	10.2 <sup>24</sup>	9.1
	$^4A_2 \rightarrow ^4B_1(\text{F})$	13.3	13.6
	$^4A_2 \rightarrow ^4E(\text{P})$	15.9	16.3
	$^4A_2 \rightarrow ^4E(\text{P})$	17.0	16.9
	$^4A_2 \rightarrow ^4A_2(\text{P})$	18.0	17.9
	$^4A_2 \rightarrow ^2G$	18.9	18.6
	$^4A_2 \rightarrow ^2G$	20.1	20.3
	$^4A_2 \rightarrow ^2G$	21.9	22.1
	ZFS, $ \Delta $		5.7 $\text{cm}^{-1}$

<sup>a</sup> AOMX parameters ( $\text{cm}^{-1}$ ):  $\epsilon_\sigma(\text{N}) = 4490$  (three imidazole nitrogens at 2.1 Å);  $\epsilon_\sigma(\text{N}) = 3000$  (1 NCS<sup>-</sup> at 1.9 Å);  $\epsilon_\sigma(\text{O}) = 2040$  (one water O at 2.2 Å);  $B = 665$ ;  $C = 4.6B$ ;  $\zeta = 146$ .

closer of the two sulfonamide oxygens at 3.2 Å. AOMX calculations were attempted assuming a five-coordinate Co(II) ligand field in an approximate trigonal-bipyramidal arrangement in which the sulfonamide oxygen occupies a distant axial position at 3.2 Å, two imidazole nitrogen's (from histidine 94 and 119) at 2.0 Å occupy equatorial positions along with the sulfonamide nitrogen at 1.9 Å and the remaining imidazole (from histidine 96) occupies the other axial position at 2.0 Å. When the  $\epsilon_\sigma$ 's were allowed to float, the one for the sulfonamide oxygen at 3.2 Å went to a very low value. A better AOMX fit was achieved if a four-coordinate structure, with the sulfonamide oxygen at 3.2 Å uncoupled (its  $\epsilon_\sigma$  set to zero), was assumed. The AOMX calculated values for nine d-d transitions and the ZFS are in good agreement with the observed values using only five AOM parameters and the four-coordinate structure. Finally, the 33  $\text{cm}^{-1}$  value determined by magnetic susceptibility for the ZFS of the human B CoCA/acetazolamide complex could not be calculated using AOMX with either the four- or five-coordinate structure unless a  $\zeta$  well above the free ion value of 515  $\text{cm}^{-1}$  were allowed. Some difference in ZFS may be attributable to the different species; however, there are additional reasons to question the 33  $\text{cm}^{-1}$  value beyond the AOMX results (*vide infra*).

Figure SI-2 shows the MCD and absorption spectra of the thiocyanate derivative of CoCA. The inset shows the fit of the VT MCD data at 416 nm ( $24.0 \times 10^3 \text{ cm}^{-1}$ , selected to avoid overlap with possibly unreacted CoCA) to eq 1 yielding a ZFS of 5.7  $\text{cm}^{-1}$ . This was an unexpectedly low value since the cobalt in CoCA/NCS<sup>-</sup> is expected to be five-coordinate since the zinc in the human carbonic anhydrase/NCS<sup>-</sup> complex is five-coordinate.<sup>3,5</sup> Therefore the ZFS measurement by VT MCD was repeated using data at 588 nm ( $17.0 \times 10^3 \text{ cm}^{-1}$ ) which resulted in the same value. The MCD spectrum has a very different pattern than is typical for four-coordinate, distorted tetrahedral Co(II). The energies and intensity pattern of the MCD bands are more typical of five-coordinate Co(II).<sup>45</sup>

Table 4 shows the AOMX calculation summary using the crystal structure of the native zinc human carbonic anhydrase II complex with thiocyanate reported by Eriksson *et al.*<sup>5</sup> The structure is in between a trigonal bipyramid and a square pyramid in terms of the ligand-metal-ligand bond angles, but the d-d transitions in CoCA/NCS<sup>-</sup> have a pattern more typically  $C_{4v}$  than  $D_{3h}$  so we chose to reference the origin of the assigned bands in the MCD and absorption spectra in Table 4 to the ideal  $C_{4v}$  geometry (this does not affect the AOMX calculation in any way since we use the actual coordinates of

(45) Kaden, T. A.; Holmquist, B.; Vallee, B. L. *Inorg. Chem.* **1974**, *13*, 2585-2590.

the atoms in the calculations, it only changes the symmetry labels). The fit results are excellent for the d–d bands (the intense bands above 23 000 cm<sup>-1</sup> are presumed to be charge transfer bands, which AOMX does not calculate), but the calculated ZFS of 7.2 cm<sup>-1</sup> does not agree with the experimental value of 5.7 cm<sup>-1</sup> (within 20%), even with a very low value of the spin–orbit coupling constant of 146 cm<sup>-1</sup>. This may be attributable to the extreme sensitivity of the calculated ZFS to equatorial bond angles in five-coordinate species (*vide infra*). Nevertheless both the calculated and experimental values for the ZFS are considerably below the lower limit of 20 cm<sup>-1</sup> set for five-coordinate Co(II) by the CN/ZFS correlation.<sup>12</sup>

Shown in Figure SI-3 is the MCD and absorption spectra of CoCA at pH 5.9. The inset to Figure SI-3 shows the fit of the VT MCD data at 560 nm (17.9 × 10<sup>3</sup> cm<sup>-1</sup>) to eq 1 to give a ZFS of 6.1 cm<sup>-1</sup>. Unfortunately there is no crystal structure of any of the low pH forms of CoCA. The structures of some of the low pH isozymes of human ZnCA have been reported, but the number of first-shell water molecules is unclear.<sup>43,46,47</sup> It is thought from a variety of investigations that the Co(II) in low pH CoCA is five-coordinate.<sup>1</sup> Supportive of this is the shape of the MCD spectrum of low pH CoCA which is close to that of CoCA/NCS<sup>-</sup> and typical of five-coordinate Co(II) complexes in general;<sup>45</sup> however, the 6.1 cm<sup>-1</sup> value for the ZFS is again well below the lower CN/ZFS correlation limit for five-coordinate Co(II).<sup>12</sup> AOMX calculations were not done on low pH CoCA because no structural data are available.

**Co Liver Alcohol Dehydrogenase Derivatives.** Werth *et al.* have recently reported the MCD spectra and ZFS of Co(c)-Zn(n)LADH, Zn(c)Co(n)LADH, and the Co(c)Zn(n)LADH/NAD<sup>+</sup>/pyrazole ternary complex.<sup>16</sup> Our spectra and fits of the VT MCD data are shown in Figures SI-4–6. We include our results to illustrate two points, one being that there is discrepancy between ZFS's determined by the same VT MCD method, and two, the advantage of MCD to “tune in” to specific bands so that the ZFS can be determined in mixed metal or contaminated samples. Our result of 30 cm<sup>-1</sup> for the ZFS of Co(c)Zn(n)LADH agrees well with that of 33 cm<sup>-1</sup> determined by Werth *et al.* However our result of 3.3 cm<sup>-1</sup> differs by more than 20% from the value of 7 cm<sup>-1</sup> reported by Werth *et al.* for Zn(c)Co(n)LADH. We do not consider our results to be fully reliable however because we were unable to completely isolate pure forms of the Co(c)Zn(n)LADH and Zn(c)Co(n)LADH and were able only to get mixtures. Thus our MCD spectra of these as well as the ternary complex were of mixtures having cobalt in both the catalytic and structural sites. Furthermore, the signal-to-noise in our spectra did not allow us to gather data other than at 0.5 T, which reduces our confidence in the determined ZFS's (the ZFS for most of our examples are averages of five separate determinations at five different magnetic fields). The ZFS was determined to be 30 cm<sup>-1</sup> for Co(c)Zn(n)LADH using the 533 nm (18.8 × 10<sup>3</sup> cm<sup>-1</sup>) band which is unique to the catalytic site cobalt, but very weak (Werth *et al.*, 33 cm<sup>-1</sup> using the 662 nm band;<sup>16</sup> Makinen and Yim, 9.3 cm<sup>-1</sup> using the EPR, Orbach process technique<sup>14</sup>). We were also able to repeat our 30 cm<sup>-1</sup> ZFS value for Co(c)Zn(n)LADH using the 662 nm band in a sample that was approximately 90% free of cobalt in the structural site. The ZFS was determined to be 3.3 cm<sup>-1</sup> for Zn(c)Co(n)LADH using the 733 nm (13.7 × 10<sup>3</sup> cm<sup>-1</sup>) band which has moderate intensity and is unique to cobalt in the structural site (Werth *et al.*, 7 cm<sup>-1</sup> also using the 733 nm band<sup>16</sup>). Finally our Co(c)Zn(n)LADH/NAD<sup>+</sup>/pyrazole ternary complex MCD spectrum was quite poor in quality (signal-to-

**Table 5.** Summary of AOMX Calculation Results for CoLADH

derivative	origin in $T_d$	d–d transitions (cm <sup>-1</sup> /1000)	
		observed	calculated
Zn(c)Co(n)LADH <sup>a</sup>	<sup>4</sup> A <sub>2</sub> → <sup>4</sup> T <sub>1</sub> (F)	8.0 <sup>20</sup>	7.6
	<sup>4</sup> A <sub>2</sub> → <sup>4</sup> T <sub>1</sub> (P)	13.7	14.0
	<sup>4</sup> A <sub>2</sub> → <sup>4</sup> T <sub>1</sub> (P)	15.0	14.7
	<sup>4</sup> A <sub>2</sub> → <sup>4</sup> T <sub>1</sub> (P)	16.0	15.4
Co(c)Zn(n)LADH <sup>b</sup>	ZFS,  Δ	7.0 cm <sup>-1</sup>	7.3 cm <sup>-1</sup>
	<sup>4</sup> A <sub>2</sub> → <sup>4</sup> T <sub>1</sub> (F)		8.7
	<sup>4</sup> A <sub>2</sub> → <sup>4</sup> T <sub>1</sub> (P)	15.1	15.0
	<sup>4</sup> A <sub>2</sub> → <sup>4</sup> T <sub>1</sub> (P)	15.8	15.9
Co(c)Zn(n)LADH/ NAD <sup>+</sup> /pyrazole <sup>c</sup>	ZFS,  Δ	30 cm <sup>-1</sup>	30 cm <sup>-1</sup>
	<sup>4</sup> A <sub>2</sub> → <sup>4</sup> T <sub>1</sub> (F)		8.9
	<sup>4</sup> A <sub>2</sub> → <sup>4</sup> T <sub>1</sub> (P)	14.8	15.1
	<sup>4</sup> A <sub>2</sub> → <sup>4</sup> T <sub>1</sub> (P)	15.8	15.4
	<sup>4</sup> A <sub>2</sub> → <sup>4</sup> T <sub>1</sub> (P)	16.4	16.5
	ZFS,  Δ	4.8 cm <sup>-1</sup>	4.9 cm <sup>-1</sup>

<sup>a</sup> AOMX parameters (cm<sup>-1</sup>):  $\epsilon_o(S)$  = 3060 (three at 2.3 Å);  $\epsilon_o(S)$  = 3340 (one at 2.1 Å);  $B$  = 597;  $C$  = 4.6B;  $\zeta$  = 292. <sup>b</sup> AOMX parameters (cm<sup>-1</sup>):  $\epsilon_o(S)$  = 2570 (two at 2.2 Å);  $\epsilon_o(N)$  = 3810 (one at 2.2 Å);  $\epsilon_o(O)$  = 2750 (one at 2.0 Å);  $B$  = 726;  $C$  = 4.6B;  $\zeta$  = 450. <sup>c</sup> Alternate assignment has 18 200 cm<sup>-1</sup> band as part of <sup>4</sup>A<sub>2</sub> → <sup>4</sup>T<sub>1</sub>(P), but would give an  $\epsilon_o(S)$  = 4390 cm<sup>-1</sup>, unreasonably high. The 18 200 cm<sup>-1</sup> band must be a CT or doublet. <sup>d</sup> Taken from CoCA fit, see Table 2. <sup>e</sup> AOMX parameters (cm<sup>-1</sup>):  $\epsilon_o(S)$  = 2570 (one at 2.1 Å);  $\epsilon_o(S)$  = 1940 (one at 2.3 Å);  $\epsilon_o(N)$  = 3810 (one imidazole at 2.2 Å);  $\epsilon_o(N)$  = 4610 (one pyrazole at 2.0 Å);  $B$  = 685;  $C$  = 4.6B;  $\zeta$  = 278. <sup>f</sup> Alternate assignment has a 18 975 cm<sup>-1</sup> band as part of <sup>4</sup>A<sub>2</sub> → <sup>4</sup>T<sub>1</sub>(P), but would give an  $\epsilon_o(S)$  over 5000 cm<sup>-1</sup>, unreasonably high. The 18 975 cm<sup>-1</sup> band must be a CT or doublet. <sup>g</sup> If ZFS is taken as 47 or 56 cm<sup>-1</sup> (literature values, see Table 1) AOMX fit can only be made with a  $\zeta$  larger (ca. 1000 cm<sup>-1</sup>) than free ion value of 515 cm<sup>-1</sup> or by changing structure.

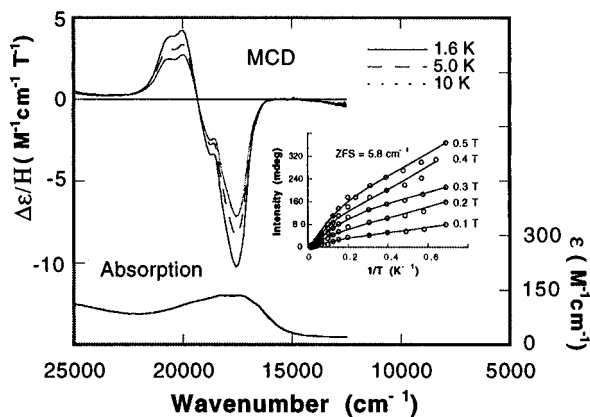
noise was low) as compared to the MCD spectrum reported by Werth *et al.*<sup>16</sup> This may account for the fact that we determined a ZFS of 4.8 cm<sup>-1</sup>. This compares poorly with the 56 cm<sup>-1</sup> value obtained by Werth *et al.*<sup>16</sup> using the 674 nm band and the value of 47 cm<sup>-1</sup> obtained by Makinen and Yim using the EPR technique (Orbach process).<sup>14</sup>

Table 5 shows the AOMX calculation results for the LADH derivatives. The structures<sup>10,11</sup> were not allowed to vary during the calculation. The values of ZFS obtained by Werth *et al.*<sup>16</sup> were used in the fits except for the Co(c)Zn(n)LADH/NAD<sup>+</sup>/pyrazole ternary complex fit. The value for ZFS of 56 cm<sup>-1</sup> obtained by Werth *et al.* resulted in an AOMX calculated spin–orbit coupling constant,  $\zeta$ , greater than 1000 cm<sup>-1</sup>, much greater than the free ion value of 515 cm<sup>-1</sup>, and physically not reasonable.<sup>15</sup> In order for a ZFS of 56 cm<sup>-1</sup> to “fit” with a reasonable spin–orbit coupling constant (between 50 and 90% of the free ion value), the ligand–Co<sup>II</sup>–ligand bond angles would have to be significantly different than those reported,<sup>11</sup> as only  $\zeta$  and bond angles have a large effect on the value of the ZFS (*vide infra*).

We were unable to get a satisfactory AOMX fit for Co(II) in the catalytic site for either the Co(c)Zn(n)LADH derivative or the Co(c)Zn(n)LADH/NAD<sup>+</sup>/pyrazole ternary complex when the 550 nm (18.2 × 10<sup>3</sup> cm<sup>-1</sup>) band in Co(c)Zn(n)LADH and the 527 nm (19.0 × 10<sup>3</sup> cm<sup>-1</sup>) band in the Co(c)Zn(n)LADH/NAD<sup>+</sup>/pyrazole ternary complex were assigned to a d–d transition derived from the <sup>4</sup>A<sub>2</sub> → <sup>4</sup>T<sub>1</sub>(P) transition in tetrahedral Co(II). The  $\epsilon_o(S)$  for the cysteine ligand was required to be approximately 25% higher than the  $\epsilon_o(N)$  from the imidazole (histidine) ligand which is not realistic. We were able to get a better AOMX fit assuming that this relatively weak band was due to a doublet or weak charge transfer transition.

Since only two d–d bands were observed for Co(c)Zn(n)LADH and only three d–d bands were observed for the Co(c)-

(46) Nair, S. K.; Christianson, D. W. *J. Am. Chem. Soc.* **1991**, *113*, 9455–(47) Hakansson, K.; Carlsson, M.; Svensson, L. A.; Liljas, A. *J. Mol. Biol.* **1992**, *227*, 1192–1204.



**Figure 2.** MCD spectra taken at 3.5 T of CoCPA, 1 mM CoCPA in 20 mM TRIS/Cl<sup>-</sup> buffer, 2 M NaCl, pH 7.4, 60% (v/v) glycerol. Absorption spectrum is of the same sample taken after the MCD experiments. Inset is the fit of the VT MCD intensity data at  $17.6 \times 10^3 \text{ cm}^{-1}$  to eq 1. Open circles are the experimental data points, and the solid line is the calculated fit to eq 1. Fit parameters at 0.5 T:  $B_0 = 74$ ;  $C_0 = 658$ ;  $B_1 = -390$ ;  $C_1 = 3865$ . Average ZFS at five fields is  $5.8 \text{ cm}^{-1}$ .

Zn(n)LADH/NAD<sup>+</sup>/pyrazole ternary complex, the  $\epsilon_\sigma$ 's could not all be independently determined. The  $\epsilon_\sigma(\text{N})$  for the imidazoles (histidine) were taken from the cobalt carbonic anhydrase fits and adjusted assuming that the ligand field strengths varied with the inverse of the square of the bond distance. The  $\epsilon_\sigma(\text{S})$  for cysteine was assumed to be the same for both Co(c)Zn(n)LADH and the Co(c)Zn(n)LADH/NAD<sup>+</sup>/pyrazole ternary complex, but it was adjusted for the different bond distances, as described above.

**Co Carboxipeptidase A Derivatives.** Figure 2 shows the MCD and absorption spectra of CoCPA, and the inset shows the fit of the VT MCD data at  $569 \text{ nm}$  ( $17.6 \times 10^3 \text{ cm}^{-1}$ ) to eq 1 to give a ZFS of  $5.8 \text{ cm}^{-1}$ . While this value is more than 20% lower than the  $8.3 \text{ cm}^{-1}$  determined by the EPR technique (Orbach process),<sup>13</sup> both ZFS's are in the range four-coordinate Co(II) range suggested by the CN/ZFS correlation.<sup>12</sup> Furthermore the pattern of the MCD spectrum is clearly that of a four-coordinate Co(II) species.<sup>45</sup> However crystal structural data on CoCPA, as well as the native zinc CPA clearly show that the metal is five-coordinate.<sup>6-8</sup> The crystal structure shows that the Co(II) in CoCPA is in between a trigonal bipyramid and square pyramid in terms of L-Co-L bond angles. The cobalt ligands are the two  $\delta_1$  nitrogen's from His-196 and His-69 at  $2.1 \text{ \AA}$ , the oxygen from a water at  $2.0 \text{ \AA}$  and the  $\epsilon_1$  (at  $2.24 \text{ \AA}$ ) and  $\epsilon_2$  (at  $2.26 \text{ \AA}$ ) oxygen's from Glu-72; thus the Glu-72 carboxylate is bidentate. More recently an X-ray absorption fine structure (XAFS) analysis of single crystals and solutions of ZnCPA and CoCPA at room temperature and 100 K showed that the  $\epsilon_2$  oxygen of Glu-72 "uncouples" in room temperature or frozen solution and moves to  $2.50 \text{ \AA}$  in CoCPA and  $2.57 \text{ \AA}$  in ZnCPA.<sup>48</sup> The  $\epsilon_1$  oxygen of Glu-72 moves a bit closer at  $2.08 \text{ \AA}$ . Unfortunately XAFS does not yield angular information, so for the AOMX calculation, summarized in Table 6, we used the single crystal structure published for CoCPA,<sup>6-8</sup> but with the  $\epsilon_2$  Glu-72 uncoupled to give a distorted tetrahedral ligand field. The fit of the experimental spectrum to the calculated spectrum is excellent with a reasonable set of AOM parameters; however, in order to fit the ZFS of  $5.8 \text{ cm}^{-1}$  a very low value of  $120 \text{ cm}^{-1}$  for  $\zeta$  is required. Since the magnitude of the ZFS is very sensitive to bond angle for a given value of the spin-orbit coupling constant (*vide infra*), it is likely that

**Table 6.** Summary of AOMX Calculation Results for CoCPA<sup>a</sup>

derivative	origin in $T_d$	d-d transitions ( $\text{cm}^{-1}/1000$ )	
		observed	calculated
CoCPA with $\epsilon_2$ glutamate oxygen uncoupled <sup>b</sup>	$^4A_2 \rightarrow ^4T_1(\text{F})$	6.4 <sup>25</sup>	6.2
	$^4A_2 \rightarrow ^4T_1(\text{F})$	10.7 <sup>25</sup>	10.6
	$^4A_2 \rightarrow ^4T_1(\text{P})$	17.6	17.3
	$^4A_2 \rightarrow ^4T_1(\text{P})$	18.7	18.4
	$^4A_2 \rightarrow ^4T_1(\text{P})$	20.0	20.6
	$^4A_2 \rightarrow ^2A_1, ^2T_2(\text{G})$	20.6	20.8
ZFS, $ \Delta $		$5.8 \text{ cm}^{-1}$	$5.9 \text{ cm}^{-1}$

<sup>a</sup> AOMX parameters ( $\text{cm}^{-1}$ ):  $\epsilon_\sigma(\text{N}) = 4860$  (two imidazoles at  $2.1 \text{ \AA}$ );  $\epsilon_\sigma(\text{O}) = 3550$  (one water at  $2.0 \text{ \AA}$ );  $\epsilon_\sigma(\text{O}) = 3920$  (one glutamate oxygen ( $\epsilon_1$ ) at  $2.1 \text{ \AA}$ );  $B = 815$ ;  $C = 4.6B$ ;  $\zeta = 120$ . <sup>b</sup> XAFS has shown that one of the two glutamate oxygens uncouples in solution.<sup>48</sup>

**Table 7.** Summary of AOMX Calculation Results for CoCPA/Benzyl Succinate<sup>a</sup>

derivative	origin in $T_d$	d-d transitions ( $\text{cm}^{-1}/1000$ )	
		observed	calculated
CoCPA/BS	$^4A_2 \rightarrow ^2T_1, ^2E(\text{G})$	14.3	14.5
	$^4A_2 \rightarrow ^4T_1(\text{P})$	17.8	17.6
	$^4A_2 \rightarrow ^4T_1(\text{P})$	18.6	18.7
	$^4A_2 \rightarrow ^4T_1(\text{P})$	20.0	20.1
	$^4A_2 \rightarrow ^2A_1, ^2T_2(\text{G})$	20.7	20.5
ZFS, $ \Delta $		$6.1 \text{ cm}^{-1}$	$6.2 \text{ cm}^{-1}$

<sup>a</sup> AOMX parameters ( $\text{cm}^{-1}$ ):  $\epsilon_\sigma(\text{N}) = 5540$  (two imidazoles at  $2.0 \text{ \AA}$ );  $\epsilon_\sigma(\text{O}) = 2330$  (one BS oxygen at  $2.3 \text{ \AA}$ );  $\epsilon_\sigma(\text{O}) = 3060$  (one glutamate oxygen ( $\epsilon_2$ ) at  $2.0 \text{ \AA}$ , the  $\epsilon_1$ , axial oxygen is at  $2.8 \text{ \AA}$ );  $B = 814$ ;  $C = 4.6B$ ;  $\zeta = 203$ .

the low  $\zeta$  obtained in the AOMX fit of CoCPA is due to incorrect angular data.

Figure SI-7 shows the MCD and absorption spectra of the CoCPA complex with the L-benzyl succinate inhibitor (CoCPA/BS), and the inset shows the fit of the VT MCD data at  $538 \text{ nm}$  ( $18.6 \times 10^3 \text{ cm}^{-1}$ ) to eq 1 to give a ZFS of  $6.1 \text{ cm}^{-1}$ . This value for the ZFS is considerably lower than the  $51 \text{ cm}^{-1}$  value obtained by Kuo and Makinen on which they based their conclusion that the cobalt in CoCPA/BS inhibitor complex was five-coordinate.<sup>13</sup> Since then, the crystal structures of both the ZnCPA/BS<sup>9</sup> and CoCPA/BS<sup>6</sup> complexes have been reported and both structures have the metal to be four-coordinate. The CoCPA/BS structure has two imidazole nitrogen ligands at  $2.0 \text{ \AA}$  (from His-196 and His-69), one Glu-72 oxygen ligand at  $2.0 \text{ \AA}$  and one benzyl succinate oxygen at  $2.3 \text{ \AA}$ . Table 7 shows the results of the AOMX calculation based on this structure. The calculated and experimental d-d transitions agree well as do the calculated and experimental values for the ZFS. In order for the ZFS to be as high as  $51 \text{ cm}^{-1}$  with the reported structure,  $\zeta$  would need to be 3 times the free ion value of  $515 \text{ cm}^{-1}$ .

The MCD spectra and VT MCD data fits to eq 1 for the remaining CoCPA inhibitor complexes are shown Figures SI-8-13 (in CoCPA/gly-L-tyr, the gly-L-tyr is actually a slowly reacting substrate). Some MCD spectra and the absorption spectra of these derivatives have been previously reported, but none of them have crystal structures that have been reported, so the coordination numbers of the Co(II) are speculative.<sup>25,49</sup> We do note that in all cases the shape of the MCD spectra look more like four-coordinate Co(II), even in the high concentration inhibitor complexes, and the values of the ZFS's are little affected by the presence of inhibitors.

**Four-Coordinate Model Compounds.** The MCD, absorption or diffuse reflectance spectra of  $\text{Co}(\text{OH})_4^{2-}$ ,  $\text{Cs}_3\text{CoCl}_5$ , and

(48) Zhang, K.; Chance, B.; Auld, D. S.; Larsen, K. S.; Vallee, B. L. *Biochemistry* **1992**, *31*, 1159-1168.

(49) Bicknell, R.; Schaffer, A.; Bertini, I.; Luchinat, C.; Vallee, B. L.; Auld, D. S. *Biochemistry* **1988**, *27*, 1050-1057.



**Table 8.** Summary of AOMX Calculation Results for Bis(2,2'-di-2-imidazolylbiphenyl)cobalt(II) Dip perchlorate Triethanolate<sup>a</sup>

derivative	origin in $T_d$	d-d transitions ( $\text{cm}^{-1}/1000$ )	
		observed	calculated
bis(2,2'-di-2-imidazolylbiphenyl)cobalt(II) diperchlorate triethanol	$^4A_2 \rightarrow ^4T_1(\text{F})$	8.0	8.0
	$^4A_2 \rightarrow ^4T_1(\text{P})$	17.0	16.9
	$^4A_2 \rightarrow ^4T_1(\text{P})$	17.5	17.6
	ZFS, $ \Delta $	5.6 $\text{cm}^{-1}$	5.5 $\text{cm}^{-1}$

<sup>a</sup> AOMX parameters ( $\text{cm}^{-1}$ ):  $\epsilon_\sigma(\text{N}) = 3590$  (four imidazole nitrogens at 2.0 Å);  $B = 756$ ;  $C = 4.6B$ ;  $\zeta = 308$ .

$\text{Cs}_3\text{CoBr}_5$  as well as the VT MCD data fits to eq 1 are shown in the Figures SI-14–16. The  $\text{Cs}_3\text{CoCl}_5$  and  $\text{Cs}_3\text{CoBr}_5$  compounds were included in the original paper proposing the CN/ZFS correlation.<sup>12</sup> These have slight  $D_{2d}$  distortions from  $T_d$  so the  $m_J = \pm 3/2$  and  $m_J = \pm 1/2$  states do not mix and the sign of the ZFS still has meaning. The magnitude of the ZFS's of 5.3 and 6.6  $\text{cm}^{-1}$  obtained by VT MCD compare with 8.6 and 10.68  $\text{cm}^{-1}$  obtained by EPR measurements on  $\text{Cs}_3\text{CoCl}_5$  and  $\text{Cs}_3\text{CoBr}_5$ , respectively (the signature of the ZFS was found to be negative by EPR as well).<sup>35</sup> These values place them correctly in the four-coordinate range according to the CN/ZFS correlation. AOMX calculations have been reported for the closely related  $\text{Cs}_2\text{CoCl}_4$  and  $\text{Cs}_2\text{CoBr}_4$  species, which are complicated due to a number of partially resolved vibronic transitions.<sup>50</sup> The assignment of the MCD and absorption spectra of  $\text{Co}(\text{OH})_4^{2-}$  has been reported, and the 5.0  $\text{cm}^{-1}$  value for the ZFS is consistent with the CN/ZFS correlation.<sup>30</sup>

The MCD spectra, diffuse reflectance spectra, and ZFS fits of  $\text{Co}(\text{2-methylimidazole})_4(\text{ClO}_4)_2$ ,  $\text{Co}(\text{2-methylimidazole})_4(\text{BF}_4)_2$  (not shown, virtually identical to the perchlorate complex),  $\text{Co}(\text{imidazole})_2\text{Cl}_2$ ,  $\text{Co}(\text{thiourea})_2\text{Cl}_2$ ,  $\text{Co}(\text{thiourea})_3\text{SO}_4$ ,  $\text{Co}(\text{thiourea})_4(\text{ClO}_4)_2$  are shown in Figures SI-17–21. These model compounds are four-coordinate with nearly tetrahedral angles.<sup>51–53</sup> They were chosen to study the effects of ligand heterogeneity and ligand field strength on the ZFS. All six of the compounds have a ZFS within 1  $\text{cm}^{-1}$  of 4.8  $\text{cm}^{-1}$  (20% relative), implying that ligand heterogeneity and moderate changes in the ligand field strength are not major influences on the magnitude of the ZFS.

Bis(2,2'-di-2-imidazolylbiphenyl)cobalt(II) diperchlorate triethanolate is a four-coordinate complex with local  $D_{2d}$  symmetry. The ligands are identical imidazole ring nitrogens, two from each bidentate ligand. The bidentate ligand "bite" angle is 102°. The distortion from local tetrahedral symmetry is described by Knapp *et al.* as " $D_{2d}$  flattening" in which the dihedral planes (defined by the cobalt and one nitrogen atom from each bidentate ligand) are no longer at 90° to each other, but are reduced to 75°. The MCD and diffuse reflectance spectra are shown in Figure SI-22. The fit of the VT MCD data taken at 571 nm ( $17.5 \times 10^3 \text{ cm}^{-1}$ ) to eq 1 is shown in the inset. The resulting ZFS is 5.6  $\text{cm}^{-1}$ , well within the correlation range for four-coordinate Co(II). Table 8 summarizes the AOMX fit for bis(2,2'-di-2-imidazolylbiphenyl)cobalt(II) diperchlorate triethanolate based on the structure reported by Knapp *et al.*<sup>27</sup>

$\text{Co}[\text{SC}(\text{CH}_3)_2\text{CH}_2\text{NH}_2]_2$  has two bidentate ligands, each with a mercapto sulfur and an amine nitrogen, creating a four-coordinate Co(II) complex with local  $C_{2v}$  symmetry. The bidentate ligand "bite" angle is only 90° as compared to the

**Table 9.** Summary of AOMX Calculation Results for  $\text{Co}[\text{SC}(\text{CH}_3)_2\text{CH}_2\text{NH}_2]_2$ <sup>a</sup>

derivative	origin in $T_d$	d-d transitions ( $\text{cm}^{-1}/1000$ )	
		observed	calculated
$\text{Co}[\text{SC}(\text{CH}_3)_2\text{CH}_2\text{NH}_2]_2$	$^4A_2 \rightarrow ^4T_1(\text{F})$	6.3 <sup>26</sup>	6.6
	$^4A_2 \rightarrow ^4T_1(\text{F})$	8.3 <sup>26</sup>	8.3
	$^4A_2 \rightarrow ^4T_1(\text{F})$	9.5 <sup>26</sup>	9.4
	$^4A_2 \rightarrow ^4T_1(\text{P})$	15.6	15.6
	$^4A_2 \rightarrow ^4T_1(\text{P})$	16.1	16.1
	$^4A_2 \rightarrow ^4T_1(\text{P})$	16.9	16.9
ZFS, $ \Delta $		21 $\text{cm}^{-1}$	21 $\text{cm}^{-1}$

<sup>a</sup> AOMX parameters ( $\text{cm}^{-1}$ ):  $\epsilon_\sigma(\text{N}) = 4660$  (two amine nitrogens at 2.1 Å);  $\epsilon_\sigma(\text{S}) = 3890$  (two mercapto sulfurs at 2.3 Å);  $B = 635$ ;  $C = 4.6B$ ;  $\zeta = 315$ .

109.5° tetrahedral angle, so this structure is more pinched than the bis(2,2'-di-2-imidazolylbiphenyl)cobalt(II) diperchlorate triethanolate molecule.<sup>26</sup> The MCD and diffuse reflectance spectra of  $\text{Co}[\text{SC}(\text{CH}_3)_2\text{CH}_2\text{NH}_2]_2$  are shown in Figure SI-23. The shape of the MCD is typical of four-coordinate distorted  $T_d$  Co(II). However the VT MCD data taken at 621 nm ( $16.1 \times 10^3 \text{ cm}^{-1}$ ) when fit to eq 1 yield a ZFS of 21  $\text{cm}^{-1}$ , well above the 13  $\text{cm}^{-1}$  upper limit for four-coordinate Co(II) suggested by the CN/ZFS correlation. The particular local symmetry about the Co(II) mixes the  $m_J = \pm 3/2$  and  $m_J = \pm 1/2$  states, so the signature of the ZFS is ambiguous. Table 9 summarizes the AOMX fit for  $\text{Co}[\text{SC}(\text{CH}_3)_2\text{CH}_2\text{NH}_2]_2$  based on the structure reported by Mastropaolo *et al.*<sup>26</sup> The AOM parameter which most affects ZFS is  $\zeta$ , and it should be noted that the value of  $\zeta$  is nearly the same for  $\text{Co}[\text{SC}(\text{CH}_3)_2\text{CH}_2\text{NH}_2]_2$  and bis(2,2'-di-2-imidazolylbiphenyl)cobalt(II) diperchlorate triethanolate yet the ZFS is higher for  $\text{Co}[\text{SC}(\text{CH}_3)_2\text{CH}_2\text{NH}_2]_2$  by nearly a factor of 4. This has to do mostly with the different angular distortions from  $T_d$  symmetry and not ligand heterogeneity (*vide infra*).

The last of the four-coordinate compounds studied are the polypyrazolyl borates which present an approximate  $C_{3v}$  first coordination sphere around the Co(II). In these compounds the polypyrazolylborate ligand is tridentate except for the Co(B-(3-isopropylpyrazole)<sub>4</sub>)<sub>2</sub> complex in which the B-(3-isopropylpyrazole)<sub>4</sub> is bidentate. The third ligand is a halide or pseudohalide.<sup>36–38</sup> The structures of these are similar in the first coordination sphere so they have been treated as a group. The MCD and diffuse reflectance spectra of  $\text{Co}(\text{L}_1)\text{NCS}$  are shown in Figure SI-24; they are typical of both four-coordinate, distorted  $T_d$  Co(II) and of the other four-coordinate polypyrazolyl borates studied (Figures SI-25–29). The inset in Figure SI-24 shows the fit of the VT MCD data at 595 nm ( $16.8 \times 10^3 \text{ cm}^{-1}$ ) to eq 1 which gives a value of 3.7  $\text{cm}^{-1}$  for the ZFS. All of the four-coordinate polypyrazolyl borate Co(II) compounds gave ZFS values well within the CN/ZFS correlation limits for four-coordinate Co(II) (Table 1). The results of the AOMX calculations on two of the four-coordinate polypyrazolyl borates Co(II) compounds,  $\text{Co}(\text{L}_1)(\text{NCS})$  and  $\text{Co}(\text{L}_2)(\text{NCS})$ , are given in Table 10. The AOM parameters are very similar as would be expected for these two closely related compounds.

(50) Schmidtke, H. H.; Nover, J. *Inorg. Chim. Acta* **1995**, *240*, 231–237.

(51) Antti, C. J.; Lundberg, B. K. S. *Acta Chem. Scand.* **1972**, *26*, 3995–4000.

(52) Domiano, P.; Tiripicchio, A. *Cryst. Struct. Commun.* **1972**, *1*, 107–110.

(53) Bernarducci, E.; Bharadwaj, P.; Potenza, J. A.; Schugar, H. J. *Acta Crystallogr.* **1987**, *C43*, 1511–1514.

**Table 10.** Summary of AOMX Calculation Results for Four-Coordinate Co(II) Polypyrazoylborate Complexes

derivative	origin in $T_d$	d-d transitions ( $\text{cm}^{-1}/1000$ )	
		observed	calculated
Co(L <sub>1</sub> )(NCS) <sup>a</sup>	$^4A_2 \rightarrow ^4T_1(\text{F})$	6.4	6.5
	$^4A_2 \rightarrow ^4T_1(\text{F})$	10.6	10.6
	$^4A_2 \rightarrow ^4T_1(\text{P})$	15.7	15.7
	$^4A_2 \rightarrow ^4T_1(\text{P})$	16.8	16.8
	ZFS, $ \Delta $	3.7 $\text{cm}^{-1}$	3.6 $\text{cm}^{-1}$
Co(L <sub>2</sub> )(NCS) <sup>b</sup>	$^4A_2 \rightarrow ^4T_1(\text{F})$	6.3	6.4
	$^4A_2 \rightarrow ^4T_1(\text{F})$	10.6	10.6
	$^4A_2 \rightarrow ^4T_1(\text{P})$	15.7	15.7
	$^4A_2 \rightarrow ^4T_1(\text{P})$	16.8	16.7
	ZFS, $ \Delta $	3.7 $\text{cm}^{-1}$	3.7 $\text{cm}^{-1}$

<sup>a</sup> AOMX parameters ( $\text{cm}^{-1}$ ):  $\epsilon_\sigma(\text{N}) = 3700$  (three pyrazole nitrogens at 2.0 Å);  $\epsilon_\sigma(\text{NCS}) = 2670$  (one NCS at 1.9 Å);  $B = 736$ ;  $C = 4.6B$ ;  $\zeta = 383$ . <sup>b</sup> AOMX parameters ( $\text{cm}^{-1}$ ):  $\epsilon_\sigma(\text{N}) = 3720$  (three pyrazole nitrogens at 2.0 Å);  $\epsilon_\sigma(\text{NCS}) = 2500$  (one NCS at 1.9 Å);  $B = 740$ ;  $C = 4.6B$ ;  $\zeta = 305$ .

**Five-Coordinate Model Compounds.** Co(Et<sub>4</sub>dien)Cl<sub>2</sub> is similar to the Co(Et<sub>4</sub>dien)Br<sub>2</sub> complex reported to have a ZFS of 50  $\text{cm}^{-1}$ .<sup>12</sup> This was actually a value calculated using Wood's equation based on an ideal  $D_{3h}$  geometry and the energy of the  $^4A'_2 \rightarrow ^4E''(\text{F})$  d-d transition;<sup>54</sup> however, it is known that these complexes are in between a  $D_{3h}$  and  $C_{4v}$  geometry,<sup>32</sup> far from having ideal angles. Our VT MCD analysis of Co(Et<sub>4</sub>dien)Cl<sub>2</sub> gives a ZFS of 98  $\text{cm}^{-1}$ . The MCD and diffuse reflectance spectra and the fit to eq 1 are shown in Figure SI-30. The value of 98  $\text{cm}^{-1}$  for the ZFS puts this above the CN/ZFS correlation range of 20–50  $\text{cm}^{-1}$  for five-coordinate Co(II) and into the six-coordinate range.

The two most interesting model compounds investigated in this study are the Me<sub>6</sub>tren Co(II) complexes. These have very low ZFS values of 5.4  $\text{cm}^{-1}$  for [Co(Me<sub>6</sub>tren)Cl]Cl and 2.7  $\text{cm}^{-1}$  for [Co(Me<sub>6</sub>tren)(NCS)](NCS). These values were not expected to be this low. Werth *et al.*<sup>16</sup> had criticized the CN/ZFS correlation on the basis of their MCD studies of CoLADH, but they still concluded that while the magnitude of the ZFS cannot be used as a reliable method for distinguishing tetracoordinate from pentacoordinate Co(II), small values of the ZFS,  $|\Delta| < 20 \text{ cm}^{-1}$ , can still be used as a criteria for tetracoordinate Co(II). Furthermore the ligand field theory developed for  $D_{3h}$  Co(II) by Wood would predict that only very small spin-orbit coupling constants ( $\zeta$  about 100  $\text{cm}^{-1}$ , 19% of the free ion value) could account for these low values of ZFS.<sup>54</sup> The ZFS for [Co(Me<sub>6</sub>tren)Cl]Cl calculated with Wood's equation (eq 7) using 5800  $\text{cm}^{-1}$  for the  $^4A'_2 \rightarrow ^4E''(\text{F})$  transition and a  $\zeta$  of 432  $\text{cm}^{-1}$  (84% of the free ion value) is 43  $\text{cm}^{-1}$ , far higher than the measured 5.4  $\text{cm}^{-1}$ . Therefore we have repeated these ZFS measurements on several different preparations of the complexes, on VT MCD data from several different bands and in the case of [Co(Me<sub>6</sub>tren)Cl]Cl, which is quite soluble in ethanol/glycerol mixtures, we have repeated the ZFS determinations on solutions of the complex as well as solids prepared in mulls. Figure 3 shows the MCD and absorption spectra of [Co(Me<sub>6</sub>tren)Cl]Cl and the inset shows the fit of the VT MCD data taken at 794 nm ( $12.6 \times 10^3 \text{ cm}^{-1}$ ) to eq 1. Figure SI-31 shows the MCD and diffuse reflectance spectra of [Co(Me<sub>6</sub>tren)(NCS)](NCS) and the inset shows the fit of the VT MCD data taken at 595 nm ( $16.8 \times 10^3 \text{ cm}^{-1}$ ) to eq 1.

Table 11 summarizes the AOMX fit results for [Co(Me<sub>6</sub>tren)Cl]Cl based on the structure reported by DiVaira and Orioli<sup>55</sup>

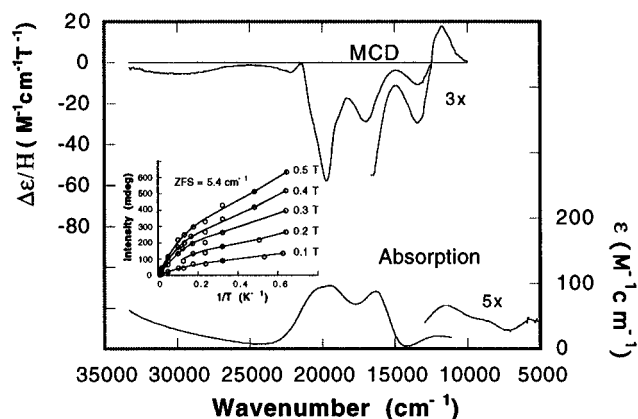


**Figure 3.** MCD spectrum of [Co(Me<sub>6</sub>tren)Cl]Cl in 50/50 (v/v) glycerol/ethanol collected at 1.0 T and 1.6 K. Absorption spectrum is the same sample as used in the MCD experiments, but at room temperature. Inset is the fit of the VT MCD intensity data at  $13.4 \times 10^3 \text{ cm}^{-1}$  to eq 1. Open circles are the experimental data points, and the solid line is the calculated fit to eq 1. Fit parameters at 0.5 T:  $B_0 = 177$ ;  $C_0 = 1260$ ;  $B_1 = -231$ ;  $C_1 = 5404$ . Average ZFS at five fields is 5.4  $\text{cm}^{-1}$ .

**Table 11.** Summary of AOMX Calculation Results for [Co(Me<sub>6</sub>tren)Cl]Cl<sup>a</sup>

derivative	origin in $D_{3h}$	d-d transition ( $\text{cm}^{-1}/1000$ )	
		observed	calculated
[Co(Me <sub>6</sub> tren)Cl]Cl	$^4A'_2 \rightarrow ^4A''_1, ^4A''_2(\text{F})$	4.1	4.5
	$^4A'_2 \rightarrow ^4E''(\text{F})$	5.8	5.2
	$^4A'_2 \rightarrow ^4E'(\text{F})$	12.6	12.8
	$^4A'_2 \rightarrow ^4A'_2(\text{P})$	16.2	16.0
	$^4A'_2 \rightarrow ^4E''(\text{P})$	19.5	19.7
ZFS, $ \Delta $		5.4 $\text{cm}^{-1}$	1.9 $\text{cm}^{-1}$

<sup>a</sup> AOMX parameters ( $\text{cm}^{-1}$ ):  $\epsilon_\sigma(\text{N}) = 4280$  (one axial amine nitrogen at 2.2 Å);  $\epsilon_\sigma(\text{N}) = 3377$  (three equatorial amine nitrogens at 2.1 Å);  $\epsilon_\sigma(\text{Cl}) = 4473$  (one axial chloride);  $\epsilon_\pi(\text{Cl}) = 790$  (one axial chloride);  $B = 740$ ;  $C = 4.6B$ ;  $\zeta = 445$ . The ZFS and resulting spin-orbit coupling constant,  $\zeta$ , are very sensitive to the angle between the equatorial ligands and axial ligands.

**Table 12.** Summary of AOMX Calculation Results for [Co(Me<sub>6</sub>tren)(NCS)](NCS)<sup>a</sup>

derivative	origin in $D_{3h}$	d-d transition ( $\text{cm}^{-1}/1000$ )	
		observed	calculated
[Co(Me <sub>6</sub> tren)NCS]NCS	$^4A'_2 \rightarrow ^4E''(\text{F})$	5.8	5.5
	$^4A'_2 \rightarrow ^4E'(\text{F})$	14.8	14.7
	$^4A'_2 \rightarrow ^4A'_2(\text{P})$	16.5	16.7
	$^4A'_2 \rightarrow ^4E''(\text{P})$	21.0	21.1
ZFS, $ \Delta $		2.7 $\text{cm}^{-1}$	2.7 $\text{cm}^{-1}$

<sup>a</sup> AOMX parameters ( $\text{cm}^{-1}$ ):  $\epsilon_\sigma(\text{N}) = 4280$  (one axial amine nitrogen at 2.2 Å);  $\epsilon_\sigma(\text{N}) = 3377$  (three equatorial amine nitrogens at 2.1 Å);  $\epsilon_\sigma(\text{NCS}) = 5840$  (one axial);  $\epsilon_\pi(\text{NCS}) = 377$  (one axial);  $B = 740$ ;  $C = 4.6B$ ;  $\zeta = 265$ . The ZFS and resulting spin-orbit coupling constant,  $\zeta$ , are very sensitive to the angle between the equatorial ligands and axial ligands.

and the assignments proposed by Bertini *et al.*<sup>56</sup> Table 12 summarizes the AOMX fit results for [Co(Me<sub>6</sub>tren)(NCS)](NCS) based on the assignments and structure proposed by Bertini *et al.*<sup>56</sup> The fit is not very satisfactory for the d-d transitions in that many AOM parameters were needed including  $\epsilon_\pi$ 's ( $\pi$  bonding parameters) for the chloride and thiocyanate; however, a surprising result is that the low ZFS's were fit by reasonable  $\zeta$ 's. In fact the calculated ZFS for the chloride is a factor of 3 lower than the observed ZFS using a  $\zeta$  which is 86% of the free ion value. This stunning result can be

(54) Wood, J. S. *J. Chem. Soc. A* **1969**, 1582–1586.(55) DiVaira, M.; Orioli, P. L. *Inorg. Chem.* **1967**, 6, 955–957.(56) Bertini, I.; Ciampolini, M.; Gatteschi, D. *Inorg. Chem.* **1973**, 12, 693–696.

understood in terms of the crystal structure of these complexes. The Me<sub>6</sub>tren ligand is a tetradentate ligand which binds to the Co(II) through four amine nitrogens, one in an axial position and three in equatorial positions, leaving the other axial position open for either a chloride or thiocyanate, making the first coordination sphere *C*<sub>3v</sub> symmetry. AOMX calculations on *C*<sub>3v</sub> molecules based on a molecule distorted from *D*<sub>3h</sub> symmetry show that the ZFS is very sensitive to the angle between the equatorial ligands and the molecular axis (when all AOM parameters are held constant including  $\zeta$ ).<sup>17b</sup> Between an angle of 60 and 90°, the ZFS can take on values from below -20 to over 60 cm<sup>-1</sup>. This angle in the Me<sub>6</sub>tren complexes is between 80 and 85°, which happens to be where the slope of the ZFS versus angle plot is at a maximum (see Figure 7 in the discussion section). Even a few tenths of degree error in the reported bond angles could account for the differences between the observed and calculated ZFS's in Tables 11 and 12.

The final three compounds studied were five-coordinate polypyrazolyl borate complexes of Co(II) which have measured ZFS's less than the 20 cm<sup>-1</sup> lower limit suggested by the CN/ZFS correlation. In Co(L<sub>1</sub>)(NO<sub>3</sub>) the complex is based on a trigonal bipyramid with the Co(II) ligand set coming from three pyrazole nitrogens and two nitrate oxygens.<sup>36</sup> The nitrate is bidentate with one oxygen ligand on the equatorial plane and the other on the axis. The Co(II) in Co(L<sub>3</sub>)(NCS)(THF) is also approximately trigonal bipyramidal with the tetrahydrofuran oxygen in one axial position and the NCS in one equatorial position; the three pyrazole nitrogens occupy the three remaining positions.<sup>36</sup> The five-coordinate Co(II) complex, Co(L<sub>2</sub>)(BBN-(pz)<sub>2</sub>), is closer to a square pyramid, with all five ligands coming from pyrazole nitrogens in polypyrazolyl borates.<sup>37</sup> The MCD, diffuse reflectance spectra and VT MCD data fits to determine the ZFS's are shown in Figures SI-32-34.

## Discussion

**The CN/ZFS Correlation.** Our results clearly show that zero-field splitting cannot be used as the sole criterion to distinguish tetracoordinate from pentacoordinate Co(II) in cobalt-substituted proteins. There is significant overlap in the range of measured ZFS for four-coordinate and five-coordinate high-spin Co(II). This is unfortunate, since measuring the ZFS of cobalt-substituted proteins in dilute aqueous solutions is relatively easy in comparison to other structural techniques such as XAFS or crystallography. Our results also show that a low ZFS ( $|\Delta| < 20$  cm<sup>-1</sup>) cannot be used as a criterion for tetracoordinate Co(II), a possibility suggested by Werth *et al.*<sup>16</sup> While the majority of our four-coordinate species were found to have ZFS's below 20 cm<sup>-1</sup>, seven out of eight of our five-coordinate species also had a ZFS below 20 cm<sup>-1</sup>.

Despite the paucity of ZFS data on high-spin Co(II) compounds in the literature, there are some reports, independent of MCD, which support our conclusions. In 1974, Cockle *et al.* determined both the sign and magnitude of the axial and rhombic components of the ZFS (*D* and *E* in eq 2) from the EPR *g*'s of two four-coordinate pyridine halide complexes of Co(II) prepared by doping Co(II) into single crystals of the zinc complexes.<sup>61</sup> The ZFS's of (C<sub>5</sub>H<sub>5</sub>N)<sub>2</sub>CoCl<sub>2</sub> and (C<sub>5</sub>H<sub>5</sub>N)<sub>2</sub>CoBr<sub>2</sub> were found to be +15 and +20 cm<sup>-1</sup>, respectively, which are both above the four-coordinate range of the CN/ZFS correlation. Cockle *et al.* also reported the ZFS's of six different sulfonamide complexes with human B, human C, and bovine cobalt carbonic anhydrases, which have been shown by X-ray crystallography to have four-coordinate metal. One human C CoCA complex was found to have a ZFS of 10 cm<sup>-1</sup>, but the other five derivatives has ZFS's ranging from 13 to 18 cm<sup>-1</sup>.<sup>61</sup>

In 1975 Duggan and Hendrickson determined the ZFS of [Co(Me<sub>6</sub>tren)Cl]Cl as approximately 10 cm<sup>-1</sup> by a detailed analysis of the temperature dependence of the magnetic susceptibility.<sup>62</sup> This value is well below the 20 cm<sup>-1</sup> minimum of the five-coordinate range proposed by the CN/ZFS correlation. Thus there is experimental evidence, independent of MCD results, that the ranges of the ZFS for four-coordinate and five-coordinate high-spin Co(II) overlap. In 1982 theoretical evidence was presented that this was indeed expected when angular distortions from ideal geometries were encountered.<sup>17b</sup>

To undo a correlation one simply needs to find examples that violate it; however, this is unsatisfactory since one would like to understand, on the basis of theory, why these exceptions occur. The CN/ZFS correlation was justified using two formula. One equation (for four-coordinate, *D*<sub>2d</sub>, Co(II)) was derived from ligand field theory by Jesson.<sup>57</sup>

$$\Delta = -\frac{8}{9}\zeta^2 \left[ \frac{1}{E(^4B_2)} - \frac{1}{E(^4E)} \right] \quad (6)$$

$\zeta$  is the spin-orbit coupling constant and *E*(<sup>4</sup>B<sub>2</sub>) and *E*(<sup>4</sup>E) are the ligand field transition energies from the ground state to the states derived from the <sup>4</sup>T<sub>2</sub>(F) split by the *D*<sub>2d</sub> distortion. The second equation (for five-coordinate, *D*<sub>3h</sub>, Co(II)) was derived from ligand field theory by Wood.<sup>54</sup>

$$\Delta = \frac{4}{3E(^4E''(F))}\zeta^2 \quad (7)$$

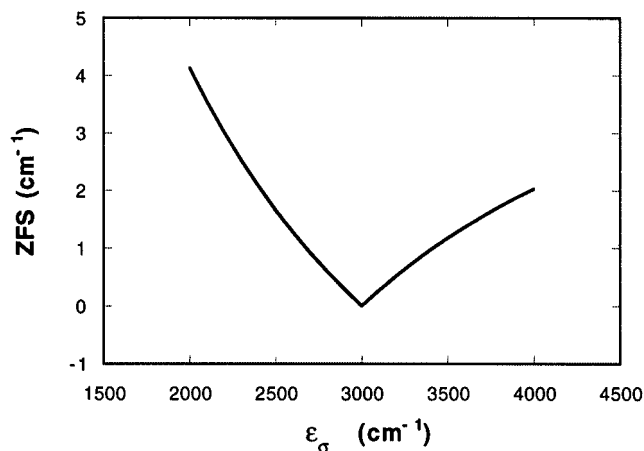
*E*(<sup>4</sup>E''(F)) is the energy of the <sup>4</sup>A'<sub>2</sub> → <sup>4</sup>E''(F) transition. These equations do not take into account angular distortions from these ideal symmetries, a situation which is more likely to represent a metalloprotein active site. The proposed CN/ZFS correlation was based in part on four-coordinate model compounds that had at least local *D*<sub>2d</sub> symmetry around the cobalt ion.<sup>12</sup> These compounds have much higher symmetry than would normally be encountered in a metalloprotein active site.

We used AOMX to calculate the ZFS for a variety of distorted four- and five-coordinate complexes to try to understand our results. What we discovered was that distortions from *T*<sub>d</sub> and *D*<sub>3h</sub> symmetries that were based on ligand heterogeneity, while contributing to the magnitude of the ZFS, do not cause the ZFS to move outside of the CN/ZFS correlation ranges unless unrealistically low values for the  $\epsilon_\sigma$ 's are selected. Two example AOMX calculations with four- and five-coordinate Co(II) in heterogeneous ligand fields are shown in Figures 4 and 5. The calculated ZFS's do not go outside of the CN/ZFS correlation ranges. Furthermore the AOM parameters *B*, *C*, and  $\epsilon_\pi$  do not, in general, cause the ZFS to go outside of the correlation ranges.

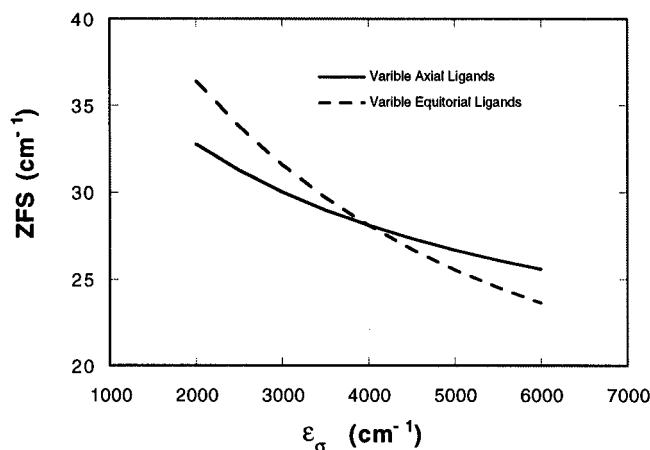
We have looked at a number of angular distortions and have found that several of these (but certainly not all) can cause the ZFS to fall outside of the correlation ranges. These results are consistent with those of Banci *et al.*<sup>17b</sup> Figure 6 shows a *C*<sub>2v</sub> distortion from *T*<sub>d</sub> symmetry, very similar to the Co[SC(CH<sub>3</sub>)<sub>2</sub>-CH<sub>2</sub>NH<sub>2</sub>]<sub>2</sub> complex which has small ( $\approx 90^\circ$ ) N(1)-Co-S(2) and N(3)-Co-S(4) bond angles. When these angles are pinched below the *T*<sub>d</sub> angle, as shown in Figure 6, the ZFS increases steeply. It should also be noted that this distortion completely mixes the *m*<sub>J</sub> = ±<sup>3</sup>/<sub>2</sub> and *m*<sub>J</sub> = ±<sup>1</sup>/<sub>2</sub> states making the sign of the ZFS ambiguous.

Figure 7 shows the results of an AOMX calculation based on distortion of a molecule having *D*<sub>3h</sub> symmetry to a molecule having *C*<sub>3v</sub> symmetry by changing the angle,  $\theta$ , that the three equatorial ligands make with the axial ligands. In this calcula-

(57) Jesson, J. P. *J. Chem. Phys.* **1968**, *48*, 161-168.



**Figure 4.** AOMX calculated effects of ligand heterogeneity on the value of ZFS in a hypothetical four-coordinate Co(II) complex. The  $T_d$  complex is distorted to  $C_{2v}$  symmetry by varying  $\epsilon_\sigma$  for two of the ligands. Angles are held at  $109.5^\circ$ . The AOM parameters are  $B = 700 \text{ cm}^{-1}$ ,  $C = 4.6B$ ,  $\epsilon_\sigma$  (variable ligands) =  $2000$  to  $4000 \text{ cm}^{-1}$ ,  $\epsilon_\sigma$  (fixed ligands) =  $3000 \text{ cm}^{-1}$ , and  $\zeta = 300 \text{ cm}^{-1}$ . At  $\epsilon_\sigma = 3000 \text{ cm}^{-1}$  the complex is  $T_d$ . This  $C_{2v}$  distortion mixes the  $m_j = \pm 3/2$  and  $m_j = \pm 1/2$  states, so the ZFS was not given signature.



**Figure 5.** AOMX calculated effects of ligand heterogeneity on the value of ZFS in a hypothetical five-coordinate Co(II) complex based on  $D_{3h}$  symmetry. The  $\epsilon_\sigma$ 's for the two axial ligands are varied while the  $\epsilon_\sigma$ 's for the equatorial ligands are fixed at  $4000 \text{ cm}^{-1}$  (solid line plot), then the  $\epsilon_\sigma$ 's for the three equatorial ligands are varied while the  $\epsilon_\sigma$ 's for the axial ligands are fixed at  $4000 \text{ cm}^{-1}$  (dashed line plot). The angles are maintained at those of a trigonal bipyramid. The AOM parameters are  $B = 700 \text{ cm}^{-1}$ ;  $C = 4.6B$ ;  $\epsilon_\sigma$  (variable ligands) =  $2000$ – $6000 \text{ cm}^{-1}$ ,  $\epsilon_\sigma$  (fixed ligands) =  $4000 \text{ cm}^{-1}$ , and  $\zeta = 300 \text{ cm}^{-1}$ .

tion all other AOM parameters were held constant. It is apparent that the value of the ZFS is extremely sensitive to  $\theta$  in the range of  $90^\circ$  to  $80^\circ$  dropping from over  $60 \text{ cm}^{-1}$  at  $90^\circ$  (out of the correlation range on the high side) to less than  $-2 \text{ cm}^{-1}$  at  $80^\circ$  (out of the correlation range on the low end). This particular distortion does not appreciably mix the  $m_j = \pm 3/2$  and  $m_j = \pm 1/2$  states, so that the ZFS has signature. This demonstrates the limitations of eq 7 (strictly for  $D_{3h}$  symmetry) which would not even allow for the possibility of a negative ZFS in a five-coordinate molecule. Figure 7 helps to explain why the  $\text{Me}_6\text{tren}$  Co(II) complexes have such low values for the ZFS as these have  $\theta$ 's in the  $80$ – $85^\circ$  range. It also serves as a possible rationalization of why the calculated ZFS for the  $[\text{Co}(\text{Me}_6\text{tren})\text{Cl}]\text{Cl}$  complex is so much lower than the observed ZFS (Table 11), despite the high  $\zeta$  used in the calculation; a small error in the angles reported in the crystal structure (which is held constant) would result in a large error in the calculated ZFS. For the  $[\text{Co}(\text{Me}_6\text{tren})(\text{NCS})](\text{NCS})$  complex the calculated and

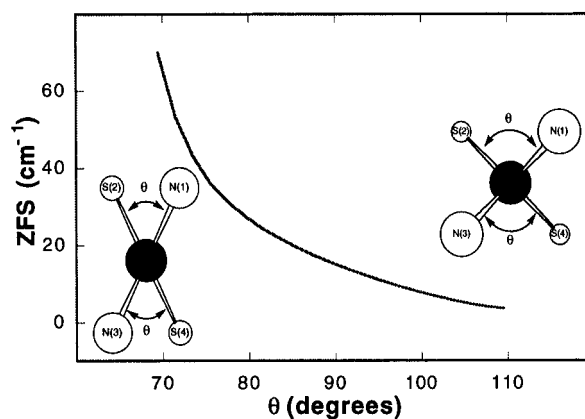


**Figure 6.** AOMX calculated effects of angular distortion on the value of the ZFS in a hypothetical four-coordinate Co(II) complex. The angles defined by  $\text{N}(1)\text{--Co--S}(4)$  and  $\text{S}(2)\text{--Co--N}(3)$  are fixed at  $109.5^\circ$ , and the angles defined by  $\text{N}(1)\text{--Co--S}(2)$  and  $\text{N}(3)\text{--Co--S}(4)$  are varied. The AOM parameters are  $B = 700 \text{ cm}^{-1}$ ,  $C = 4.6B$ ,  $\epsilon_\sigma$ ,  $\text{N}(1)$  and  $\text{N}(3) = 4000 \text{ cm}^{-1}$ ,  $\epsilon_\sigma$ ,  $\text{S}(2)$  and  $\text{S}(4) = 3000 \text{ cm}^{-1}$ , and  $\zeta = 300 \text{ cm}^{-1}$ . This hypothetical molecule is somewhat analogous to the  $\text{Co}[\text{SC}(\text{CH}_3)_2\text{CH}_2\text{NH}_2]_2$  model complex.

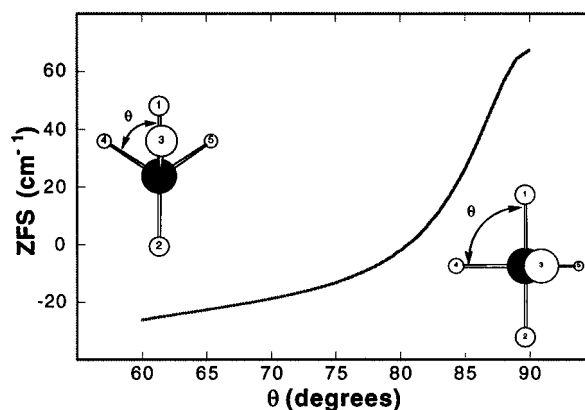


**Figure 7.** AOMX calculated effects of angular distortion on the value of ZFS in a hypothetical five-coordinate Co(II) complex. The angle that the equatorial ligands make with one axial ligand is varied. The AOM parameters are  $B = 740 \text{ cm}^{-1}$ ,  $C = 4.6B$ ,  $\epsilon_\sigma$ (equatorial ligands) =  $3400 \text{ cm}^{-1}$ ,  $\epsilon_\sigma$ (axial ligands) =  $4300 \text{ cm}^{-1}$ , and  $\zeta = 445 \text{ cm}^{-1}$ . This hypothetical molecule is somewhat analogous to the  $[\text{Co}(\text{Me}_6\text{tren})\text{X}]\text{X}$  model complexes.

observed ZFS's agree well, but only when a lower value of  $\zeta$  is used. The value of  $\zeta$  should be similar for these two complexes.

The principal application of the correlation of ZFS with Co(II) coordination number has been in the prediction of coordination number change (or lack of change) when an enzyme active site is "attacked" by a substrate or an inhibitor. An example is the  $\text{CoCA}/\text{acetazolamide}$  complex in which the sulfonamide oxygen is located  $3.2 \text{ \AA}$  from the Co(II), centered on one of the faces of the distorted tetrahedron.<sup>12–14</sup> Our results have shown that the range of ZFS for four-coordinate Co(II) complexes and the range of ZFS for five-coordinate Co(II) complexes can overlap. A telling result is shown in Figure 8. This AOMX calculation simulates the effect on the ZFS should a distorted tetrahedral Co(II) complex be "attacked" at the center of a face by a fifth ligand. In the AOMX calculation this is accomplished by increasing the  $\epsilon_\sigma$  value for the fifth ligand from 0 to some typical value ( $4000 \text{ cm}^{-1}$  for nitrogenous ligands). The angle,  $\theta$ , is fixed at  $79^\circ$  to give the attacking ligand space. Five-coordinate, distorted trigonal bipyramidal molecules with a  $\theta$  as small as  $74^\circ$  have been reported.<sup>56</sup> Figure 8 shows that in this scenario the ZFS at the four-coordinate extreme where  $\epsilon_\sigma$  of the attacking

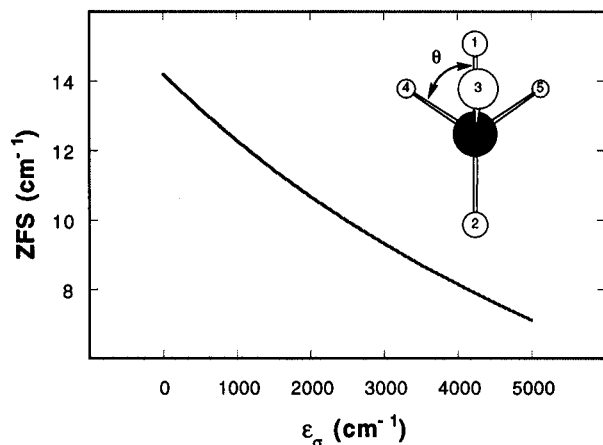


**Figure 8.** AOMX calculated effects on the value of ZFS in a hypothetical four-coordinate Co(II) molecule which is "attacked" on an open face by a fifth ligand. The angle,  $\theta$ , is fixed at  $79^\circ$ . The AOM parameters are  $B = 740 \text{ cm}^{-1}$ ,  $C = 4.6B$ ,  $\epsilon_\sigma$  (ligands 2–5) =  $4000 \text{ cm}^{-1}$ ,  $\epsilon_\sigma$  (ligand 1) =  $0\text{--}5000 \text{ cm}^{-1}$  (this is equivalent to changing the bond length of the fifth ligand from infinity to slightly shorter than normal), and  $\zeta = 400 \text{ cm}^{-1}$ .

ligand is zero is actually above the CN/ZFS correlation range at  $14 \text{ cm}^{-1}$ . As the  $\epsilon_\sigma$  is increased, which corresponds to the attacking ligand moving closer, the ZFS actually *decreases*. When  $\epsilon_\sigma$  is  $4000 \text{ cm}^{-1}$  the calculated ZFS for the five-coordinate, formally  $C_{3v}$ , species is  $8.1 \text{ cm}^{-1}$ . This is well within the tetra-coordinate Co(II) range suggested by the CN/ZFS correlation. Figure 8 suggests that there is a continuum between the allowed values of the ZFS for distorted four-coordinate and distorted five-coordinate high-spin Co(II).

**Methodologies for ZFS Measurement.** The number of Co(II) compounds that have reported ZFS's is small (Table 1), and we cannot say with certainty that the VT MCD methodology gives the correct value for the ZFS for any given complex. Our ability to repeat our own values as well as the AOM calculations which support the values of the ZFS that we have observed give us some confidence. Several of our ZFS values differ from previously published experimental measurements by more than our 20% estimate for the relative standard deviation. These differences are less than a factor of 2 in all but the CoLADH and CoCPA/BS examples, and for the purposes of testing the CN/ZFS correlation ranges, we feel that this is adequate agreement. The question arises, however, as to the relative strengths and weaknesses of the different methods used to measure ZFS.

Four experimental methods have been used to generate the ZFS values listed in Table 1. VT MCD, magnetic susceptibility, temperature dependence of the saturation behavior of the EPR signal (Orbach process), and calculation of  $D$  (and  $E$ ) from  $g_x$ ,  $g_y$ ,  $g_z$  determined by EPR and spin-orbit coupling constant ( $D = \lambda/2[g_z - 1/2(g_x + g_y)]$ ;  $E = \lambda/4(g_x - g_y)$ ).<sup>63</sup> Two theoretical approaches have been used to calculate the ZFS. Jesson's<sup>57</sup> and Wood's<sup>54</sup> equations for ideal  $D_{2d}$  and  $D_{3h}$  molecules and the AOM ligand-field calculations.

When the ZFS is determined from the EPR  $g$ 's, the relationship of the  $g$ 's to the ZFS is derived from ligand field theory. There is an implicit assumption of geometry when using these equations with  $d^7$  ions since LS coupling of low lying states with the ground state can make these equations inapplicable.<sup>63</sup> Severe tetragonal distortions from octahedral symmetry and moderate distortions from the five-coordinate geometries of  $D_{3h}$  and  $C_{4v}$  can create this situation. When Cockle *et al.* used this method to determine the ZFS's of CoCA/sulfonamide complexes and pyridine halide Co(II) complexes, they assumed that the

high-spin Co(II) was in a moderately distorted tetrahedral environment.<sup>61</sup>

The EPR, Orbach process, technique has been described in some detail and is based on the temperature dependence of the saturation behavior of an EPR resonance.<sup>12,64,65</sup> Two major limitations of this method are that compounds with spin-lattice relaxation rates too fast at liquid helium temperatures cannot be measured, and paramagnetic impurities may alter the temperature dependence of the cobalt relaxation.<sup>65</sup> The second limitation could be a serious limitation in metal-substituted proteins in which the presence or absence of adventitiously bound metals may be unknown. This may account for the large difference in the ZFS's ( $6.1$  by VT MCD versus  $51 \text{ cm}^{-1}$  by EPR, Orbach process) observed for the benzyl succinate complex of CoCPA (Table 1). The Orbach process must be regarded as a bulk sample technique much like magnetic susceptibility despite the fact that a single resonance line is used in the analysis. Both EPR-based methods can be limited when the ZFS is large compared to  $kT$  and the  $\pm^{3/2}$  doublet is lower than the  $\pm^{1/2}$  doublet. The fast spin-relaxation phenomenon of high-spin Co(II) requires that the temperature be kept low (typically  $20 \text{ K}$  or less) to observe signals, so  $kT$  is always small. In these cases the only thermally accessible transition is the forbidden  $-^{3/2} \rightarrow ^{3/2}$  transition which may be too weak to observe.<sup>66</sup>

The temperature dependence of the magnetic susceptibility is the oldest technique that has been used to measure the ZFS, but it also has limitations, which if not recognized, could lead to erroneous ZFS values. Magnetic susceptibility is a bulk technique, so the amount and type of each paramagnetic species in the sample must be known, for an accurate analysis. This could be a problem in proteins which may have multiple, nonspecific, binding sites for metals. Once an accurate data set is obtained, the numerical analysis of the data can affect the value of the resulting ZFS. Duggan and Hendrickson have shown that the ZFS of  $[\text{Co}(\text{Me}_6\text{tren})\text{Cl}]\text{Cl}$ , which they estimated to be  $10 \text{ cm}^{-1}$ , depends on the theoretical model used to fit the susceptibility data.<sup>62</sup> They found that both spin-orbit coupling of the ground state with higher energy states and crystal field mixing of the  $^4A_2'(\text{F})$  ground state with the  $^4A_2'(\text{P})$  excited state were necessary to properly fit the susceptibility data at all temperatures. Furthermore both of these effects were found to contribute differently to the determined value of the ZFS which could be as low as  $0$  or as high as  $58 \text{ cm}^{-1}$  if these effects were not both taken into account. This implies that susceptibility cannot be used to determine the ZFS unless both knowledge of the symmetry and knowledge of the energy levels of the molecule are known. These effects were not considered in the fit of the susceptibility data of the human B CoCA/acetazolamide complex which resulted in a ZFS of  $33 \text{ cm}^{-1}$ .<sup>44</sup> These researchers reported that the room temperature susceptibility data was not accurately fit with the ZFS of  $33 \text{ cm}^{-1}$  supporting the possibility that the theoretical model was incomplete. The ZFS determined from the EPR  $g$ 's on the same human B CoCA complex was  $17 \text{ cm}^{-1}$ .<sup>61</sup> These can be compared to the bovine CoCA/acetazolamide complex which had a ZFS determined by EPR  $g$ 's to be  $13 \text{ cm}^{-1}$  and by VT MCD to be  $11 \text{ cm}^{-1}$ .<sup>61</sup>

The VT MCD technique to determine ZFS is not without problems or limitations. The accuracy of the method is limited by the ability to measure temperatures from  $1.5$  to  $150 \text{ K}$  accurately (a limitation of the magnetic susceptibility and Orbach methods as well), the intensity of the MCD signal which affects the accuracy of the intensity measurements, and the ability to form a high-quality optical glass of dissolved samples (a problem with our CoLADH/NAD<sup>+</sup>/pyrazole complex sample). All

distorted tetrahedral and most of the five- and six-coordinate high-spin Co(II) complexes have very intense MCD spectra which still have measurable intensities above 200 K, so MCD signal strength is not generally a significant source of error in the measured ZFS for Co(II) compounds. The VT MCD technique is limited at the very low end ( $\approx 1 \text{ cm}^{-1}$ ) and very high end ( $\approx 100 \text{ cm}^{-1}$ ) of the ZFS range. At the low ZFS extreme, energy gaps less than  $kT$  (usually about  $1 \text{ cm}^{-1}$ ) cannot be measured. Also at small ZFS, the Zeeman splitting of the  $\pm^{3/2}$  and  $\pm^{1/2}$  Kramers doublets may cause the split states to cross at higher magnetic fields and the fit to eq 1 would no longer be valid. This is why the lowest possible magnetic fields are used in the VT MCD analysis. If an effective  $g$  of 6 is chosen for the  $\pm^{3/2}$  doublet and an effective  $g$  of 2 is chosen for the  $\pm^{1/2}$  doublet, the doublet states would start to cross at a 0.5 T applied magnetic field if the ZFS were about  $1 \text{ cm}^{-1}$ . This is essentially the limit imposed by  $kT$ . Our measured ZFS's are well above this limit and were usually measured with applied fields well below 0.5 T. At the high end of the ZFS range the C-term MCD signal decreases rapidly at temperatures above 100 K. If the energy gap is about  $100 \text{ cm}^{-1}$  temperatures well above 100 K are needed to significantly populate the upper doublet. An additional problem with solutions is that the 50/50 glycerol/water phase transition is at about 160 K. Milled solids do not have this problem. The ability of the VT MCD technique to accurately measure a high ZFS value will be very sample dependent. The "sweet" spot of the VT MCD technique falls in the  $5\text{--}25 \text{ cm}^{-1}$  range which happens to correspond to the range of overlap between four- and five-coordinate Co(II) complexes.

VT MCD has some distinct advantages over the other techniques for ZFS determination. It is not a bulk sample technique. A single MCD transition allows that specific ground state to be probed. Additional transitions in the same sample arising from the same ground state can be used for verification of the ZFS. Additional MCD transitions in the sample which arise from ground states of a different metal can be used to measure its ZFS. Only a metal which has an overlapping MCD transition will interfere with the ZFS measurement. This is an advantage when working with metal-substituted proteins where small amounts of adventitiously bound metals must be considered the rule rather than the exception. Another advantage of the VT MCD technique is that the fit model for the data is a simple Boltzmann population model. There is no presumption of (or need to know) structure, higher lying excited states, or spin-relaxation models. There is no reliance on ligand-field theory models or spin-Hamiltonians to fit the data. The only requirement is that the number of thermally accessible energy gaps is known (always one for high-spin Co(II), regardless of structure). This advantage would be particularly useful when dealing with proteins of unknown structure.

**AOM Calculations.** The ranges of the ligand-field parameters  $B$  and  $\epsilon_g$  in Tables 2–12 are well within reason on the basis of published parameters;<sup>17</sup> however, the spin-orbit coupling constant,  $\zeta$ , varies from 23 to 87% of the free ion value.<sup>60</sup> The calculated ZFS is proportional to the square of the spin-orbit coupling constant,  $\zeta$ , but it is also very sensitive to the bond angles which have been treated as accurately known constants. The free ion value for  $\zeta$  is  $515 \text{ cm}^{-1}$  but will be reduced in molecules due to covalency.<sup>15</sup> Values for ZFS on the low end can be calculated using AOMX if  $\zeta$  is allowed to be small, but how small is still realistic? Cotton has published magnetic susceptibility results on several tetrahedral Co(II) complexes which give values of  $\zeta$  between 73% and 96% of

the free ion value.<sup>58</sup> Duggan and Hendrickson noted that for  $[\text{Co}(\text{Me}_6\text{tren})\text{Cl}]\text{Cl}$  a value for the spin-orbit coupling constant which is 56% of the free ion value was needed to fit their data; whereas, in our AOMX calculation a value of  $\zeta$  84% of the free ion value resulted in a low calculated ZFS (Table 11). The range of experimentally determined spin-orbit coupling constants for four- and five-coordinate Co(II) is 56% to 96% of the free ion value, and one value of 110% was reported for a six-coordinate Co(II) complex.<sup>67</sup> Kirk *et al.* have recently published a study of Cr(III) complexes in which they calculate  $\zeta$  to be  $100 \text{ cm}^{-1}$ , 36% of the free ion value.<sup>59</sup> Wood has also noted that covalency effects tend to be extreme in trigonal bipyramid molecules distorted to  $C_{3v}$ .<sup>68,69</sup> In light of these results, values of  $\zeta$  as low as 30–40% of the free ion value may be physically meaningful; however, some researchers have assumed that  $\zeta$  will be near to 80% of the free ion value in all Co(II) complexes.<sup>12</sup>

The lowest AOMX calculated  $\zeta$  is  $120 \text{ cm}^{-1}$  for the CoCPA derivative (Table 6). This protein has been shown to be five-coordinate in the crystalline form but four-coordinate in solution by XAFS.<sup>48</sup> The bond angles used in the AOMX calculation were taken from the crystal structure since no angular data are available from the XAFS, and it is likely that the calculated  $\zeta$  is wrong because of erroneous bond angle data. The next lowest calculated  $\zeta$  of  $146 \text{ cm}^{-1}$  is for the five-coordinate CoCA/NCS<sup>-</sup> protein complex (Table 4). This active site has a structure angularly distorted between a square pyramid and a trigonal bipyramid. Like the example shown in Figure 7, this type of distortion creates a situation where the ZFS is very sensitive to the bond angles. In the AOMX calculation, the bond angles and ZFS are fixed, and the only way the program can fit the ZFS is to adjust  $\zeta$ . A large error in the ZFS results in only a small change in the calculated  $\zeta$ . For example, if the ZFS were 300% higher ( $17 \text{ cm}^{-1}$  rather than  $5.7 \text{ cm}^{-1}$ ) in the CoCPA/NCS<sup>-</sup> complex, and the structure were held the same, the calculated  $\zeta$  would be only  $250 \text{ cm}^{-1}$ , still only 49% of the free ion value. On the other hand if some of the bond angles are allowed to vary as little as  $2^\circ$ , a calculated ZFS of  $5.7 \text{ cm}^{-1}$  can be achieved with a  $\zeta$  of  $412 \text{ cm}^{-1}$ , 80% of the free ion value.

The AOMX calculation results for five-coordinate Co(II) Me<sub>6</sub>tren complexes in Tables 11 and 12 also illustrate the extreme sensitivity of the calculated ZFS and  $\zeta$  to bond angles. There is no plausible reason for the closely related  $[\text{Co}(\text{Me}_6\text{tren})\text{Cl}]\text{Cl}$  and  $[\text{Co}(\text{Me}_6\text{tren})\text{NCS}]\text{NCS}$  complexes to have  $\zeta$ 's as different as 445 and  $265 \text{ cm}^{-1}$  for the chloride and thiocyanate, respectively. If the AOMX program were "forced" to fit the experimental ZFS in  $[\text{Co}(\text{Me}_6\text{tren})\text{Cl}]\text{Cl}$  without

(58) Cotton, F. A.; Goodgame, D. M. L.; Goodgame, M. *J. Am. Chem. Soc.* **1961**, *83*, 4690–4699.

(59) Kirk, A. D.; Hoggard, P.; Gudel, H. U. *Inorg. Chim. Acta* **1995**, *238*, 45–55.

(60) Lever, A. B. P. *Inorganic Electronic Spectroscopy*, 2nd ed.; Elsevier: Amsterdam, 1984; pp 763–764.

(61) Cockle, S. A.; Lindskog, S.; Grell, E. *Biochem. J.* **1974**, *143*, 703–715.

(62) Duggan, D. M.; Hendrickson, D. N. *Inorg. Chem.* **1975**, *14*, 1944–1956.

(63) McGarvey, B. R. In *Transition Metal Chemistry*; Carlin, R. L., Ed.; Marcel Dekker: New York, 1966; page 118.

(64) Yim, M. B.; Kuo, L. C.; Makinen, M. W. *J. Magn. Res.* **1982**, *46*, 247–256.

(65) Carlin, R. L. *Magnetochemistry*; Springer-Verlag: Berlin: 1986; p 303.

(66) Fukui, K.; Kojima, N.; Ohya-Nishiguchi, H.; Hirota, N. *Inorg. Chem.* **1992**, *31*, 1338–1344.

(67) Mackey, D. J.; Evans, S. V.; McMeeking, R. F. *J. Chem. Soc., Dalton Trans.* **1978**, 160–165.

(68) Wood, J. S. *Inorg. Chem.* **1968**, *7*, 852–859.

(69) Wood, J. S.; Green, P. T. *Inorg. Chem.* **1969**, *8*, 491–497.

altering the angles obtained from the crystal structure and irrespective of the weighing factors and the fit function given in eqs 4 and 5, the resulting  $\zeta$  would end up being about  $750\text{ cm}^{-1}$ , 146% of the free ion value. Another way of looking at this problem is to calculate the ZFS's of these two complexes with a fixed value of  $\zeta$  of  $412\text{ cm}^{-1}$  or 80% of the free ion value and keeping the structures and all the other AOM parameters the same. This results in a calculated ZFS of  $1.6\text{ cm}^{-1}$  for  $[\text{Co}(\text{Me}_6\text{tren})\text{Cl}]\text{Cl}$  and  $6.4\text{ cm}^{-1}$  for  $[\text{Co}(\text{Me}_6\text{tren})\text{-NCS}]\text{NCS}$ . Clearly the angles must be slightly different than reported in the structures. It is also interesting to note that even if one assumes a large  $\zeta$  (80% of the free ion value) the calculated ZFS's are well below those predicted by the CN/ZFS correlation.

Since ZFS is sensitive to both  $\zeta$  (covalency) and bond angles, it cannot by itself be used for structural inferences. However in combination with observed ligand field transitions, ligand field calculations and techniques such as XAFS (providing coordination number), ZFS may prove useful in defining accurate solution structures for Co(II)-substituted protein active sites. This is clearly the direction that proponents of AOM calculations have given as a goal.<sup>18</sup>

### Summary and Conclusions

The magnitude of the zero-field splitting (ZFS) cannot be used as the sole indicator of coordination number in Co(II) complexes or Co(II)-substituted zinc enzymes. The magnitude of the ZFS is not very sensitive to ligand heterogeneity but can be very sensitive to bond angles. Since protein active sites are

in general highly angularly distorted from ideal four- or five-coordinate geometries, ZFS is rendered useless as a sole indicator of coordination number. These conclusions are based on the determination of the magnitude of the ZFS using VT MCD in a number of four- and five-coordinate Co(II) model complexes and Co(II)-substituted zinc enzymes of known geometry. The experimental results are supported by AOM calculations.

**Acknowledgment.** The authors gratefully acknowledge financial support from the The Petroleum Research Fund (ACS-PRF no. 26582-B3), The National Institutes of Health (R15 GM49398-01) and The Camille and Henry Dreyfus Foundation (HT-94-030, JAL Henry Dreyfus Teacher-Scholar). The authors also acknowledge Drs. J. S. Thompson and S. Trofimenko of E. I. du Pont de Nemours and Company, Wilmington, DE, for kindly providing the polypyrazolyl borate Co(II) complexes. J.A.L. further acknowledges Professor E. I. Solomon of Stanford University and the National Science Foundation NSF/ROA program for sabbatical leave support in 1992–1993.

**Supporting Information Available:** Thirty-four additional figures showing MCD and absorption spectra as well and fits of VT MCD data to eq 1 are available (17 pages). See any current masthead page for ordering and Internet access instructions.

JA963555W